Green Synthesis of Silver and Zinc Oxide Nanoparticles using *Mimusops elengi* Linn. Leaf Extract and Cytotoxicity

Selly Arvinda Rakhman

A Thesis Submitted in Fulfillment of the Requirements for the Degree of Master of Science in Applied Chemistry

Prince of Songkla University

2020

Thesis Title	Green Synthesis of Silver and Zinc Oxide Nanoparticles using *Mimusops elengi* Linn. Leaf Extract and Cytotoxicity
Author	Miss Selly Arvinda Rakhman
Major Program	Applied Chemistry

Major Advisor

……..……....

(Dr. Weeraya Khummueng)

Co-advisor

……..……....

(Dr. Charoen Pakhathirathien)

……..……....

(Dr. Tanyarath Utaipan)

Examining Committee

……..... Chairperson

(Asst. Prof. Dr. Saowapa Chotisuwan)

……..……...

(Asst. Prof. Dr. Anan Athipornchai)

……..……...

(Dr. Weeraya Khummueng)

……..……...

(Dr. Charoen Pakhathirathien)

……..……...

(Dr. Tanyarath Utaipan)

The Graduate School, Prince of Songkla University, has approved this thesis as fulfillment of the requirements for the Master of Science Degree in Applied Chemistry.

……..……...

(Prof. Dr. Damrongsak Faroongsarng)

Dean of Graduate School

This is to certify that the work here submitted is the result of the candidate's own investigations. Due acknowledgment has been made of any assistance received.

……..…..…….……....

(Dr. Weeraya Khummueng)

Major Advisor

……..…….…….……....

(Miss Selly Arvinda Rakhman)

Candidate

I hereby certify that this work has not been accepted in substance for any degree and is not being currently submitted in candidature for any degree.

……..…….…….……....

(Miss Selly Arvinda Rakhman)

Candidate

Thesis Title Green Synthesis of Silver and Zinc Oxide Nanoparticles using *Mimusops elengi* Linn. Leaf Extract and Cytotoxicity
Author Miss Selly Arvinda Rakhman
Major Program Applied Chemistry
Academic Year 2020

ABSTRACT

Green synthesis is one of method for synthesize nanoparticles using biological material. Metal nanoparticles in this research will be produced by synthesis of *M. elengi* leaf extract that combine with metal precursor to make silver nanoparticle (AgNP) and zinc oxide nanoparticle (ZnONP). Characterization of metal nanoparticle used FTIR, UV-Visible spectrophotometer, XRD and TEM. Application of metal nanoparticle were antioxidant and cytotoxicity against colon cancer, Caco-2.

Silver nanoparticles (AgNP) revealed that it has mostly round shapes with the particle size of AgNP was 16.84 nm – 33.67 nm or the average of particle size was 22.12 nm. Zinc Oxide Nanoparticles (ZnONP) characterization revealed that it has mostly round shapes with the particle size was 18.56 – 40.04 nm or the particle size was 28.44 nm in average.

Application as antioxidant based on EC_{50} value for extract, AgNP and ZnONP by DPPH assay get the result 139.97 mg/L, 237.33 mg/L and 5380.20 mg/L. The other method by ABTS assay have the result 37.34 mg/L, 215.45 mg/L and 2785.41 mg/L. The last method for FRAP assay showed the value 4.03 µM FE/ mM extract, 0.97 µM FE/ mg extract and 0.09 µM FE/ mg extract. Cytotoxicity of extract and nanoparticles (AgNP and ZnONP) showed that only extract at 2000 ppm has potential against colon cancer (Caco-2 cell) but no effect of nanoparticles (AgNP and ZnONP).

Keywords: Nanoparticle, *Mimusops elengi*, green synthesis, antioxidant, cytotoxicity

ACKNOWLEDGMENT

I would like to gratefully acknowledge to Prince of Songkla University (PSU) for Thailand's Education Hub for Southern Region of ASEAN Countries (TEH-AC) scholarship for allowing me to continue study as master student in PSU Pattani, Thailand from 2018 to 2020 and to Graduate School of PSU for providing the thesis grant that supporting my thesis research.

I would like to render my deep sincere appreciation to my major advisor, Dr. Weeraya Khummueng and to all my co-advisor, Dr. Charoen Pakhathirathien and Dr. Tanyarath Utaipan for providing guidance and encouregement throughout this research. It was a great honor to work and to study under their guidance. I extended my heartfelt gratitude to all the lecturer in Chemistry Divisions for the learning, discussions and suggestions and to all the staffs at the Chemistry Division, Faculty of Science and Technology for all the supports. I feel blessed to this faculty members.

I would like to express my warm gratitude to all my friends in the research and study for their companionship, supports and helps. Finally, i would like to dedicate this work to my parents, my beloved family for always showering me a huge of love, prayers, caring and courage whole through my master journeys.

Selly Arvinda Rakhman

TABLE OF CONTENTS

LIST OF TABLES

LIST OF FIGURES

LIST OF ABBREVIATIONS AND SYMBOLS

Ag	=	Argentum (Silver)
AgNP	=	Silver Nanoparticle
ABTS	=	2,2′-Azino-bis(3-ethylbenzothiazoline-6-sulfonic acid) diammonium salt
ANOVA	=	Analysis of Variance
Caco-2	=	a continuous line of heterogeneous human epithelial colorectal adenocarcinoma cells
CE	=	Catechin equivalent
DPPH	=	2,2-Diphenyl-1-picrylhydrazyl
EC_{50}	=	Half maximal effective concentration
FE	=	Ferric equivalent
FRAP	=	Ferric reducing antioxidant power
FTIR	=	Fourier-transform infrared spectroscopy
GAE	=	Gallic Acid Equivalent
IC_{50}	=	The half maximal inhibitory concentration
JCPDS	=	Joint Committee on Powder Diffraction Standards
M. elengi	=	*Mimusops elengi* Linn.
MTT	=	Tetrazolium salt 3-(4, 5-dimethylthiazol-2-yl)-2, 5-diphenyltetrazolium bromide
NP	=	Nanoparticle
OH^-	=	Hydroxide
PBS	=	Phosphate buffered saline
pH	=	Power of hydrogen
ROS	=	Reactive oxygen species
SPR	=	Surface plasmon resonance
TEAC	=	Trolox equivalent antioxidant capacity
TFC	=	Total flavonoid content
TPC	=	Total phenolic content
TPTZ	=	2,4,6-Tri(2-pyridyl)-s-triazine

UV-Vis	=	Ultra violet-visible
XRD	=	X-ray diffraction
Zn	=	Zinc
ZnO	=	Zinc oxide
ZnONP	=	Zinc oxide nanoparticle

CHAPTER 1
INTRODUCTION

1.1 Research background

Nowadays nanotechnology has become important and exciting fields in science and technology. Nano in the word nanotechnology means the size of particle in a billionth (1×10^{-9}) meter. Actually, nanostructures have existed on earth as long as life itself (Poole et al., 2003). One of nanomaterial form is nanoparticle. Nanoparticle is object that has a structure with homogenous physicochemical properties. Nanoparticle can be made from metal solution that react with bio agent like from part of plant extract by green synthesis method, then produce metal nanoparticle (Lane, 2000).

Green synthesis nanoparticle from metal ion and extract plant widely used in science and technology field because it can improve properties in size, distribution and morphology than particle in the bulk. Green synthesis of nanoparticle in this research can make the experiment more effective and efficient because use less energy. Silver nanoparticles (AgNP) have strong characteristic in shape, size and distribution. It became affected by reducing and stabilizing agents. Zinc oxide nanoparticles (ZnONP) are metal oxide nanoparticles that can apply in biomedical field such as diagnosis to treatment. AgNP and ZnONP also can be applied for bioimaging, biosensors, antimicrobial, antioxidant, anticancer action, drug and gene delivery (Sruthi et al, 2018).

Plant extract make role important in green synthesis nanoparticles as reducing and capping agent for metal ions. *Mimusops elengi* (*M. elengi*) is one of plant that abundance in Southeast East Asian like in Indonesia, Malaysia and Thailand. It is belonging to family *Sapotaceae*, a medicinal plant which has abundance of polyphenols and tannins has activity as antioxidant and anticancer. (Gopalkhrisnan and Shimpi, 2012).

There are many antioxidants and anticancer from synthetic product, but if it has been used in long period, it can be harmful to human health. Natural

product is the alternative solution for using as antioxidant and anticancer which safer to use.

The effect of excessive free radical reaction in human body at high level is cancer disease. The most common forms of cancer are colon, lung, breast and prostate cancer. Anti-cancer drugs destroy cancer cells by stopping growth or multiplication at some point in their life cycles (Sisodiya, 2013).

This study is important because it was aimed to investigate antioxidant and cytotoxicity activity from natural resource which is safer to use and not harmful for human. It is economist because it is easy to get and easy to make. Particle in nano size can spread in widely surface, high viscosity and more reactive than particle in bulk. Beside that it's also eco-friendly because using renewable material which design for degradation, safer chemical, prevents waste and pollution to the environment.

1.2 Research objectives

The objective of this study is to synthesize silver nanoparticle and zinc oxide nanoparticle using *M. elengi* Linn. leaf extract then investigate the potential of antioxidant and cytotoxicity toward different cell lines.

1.3 Expected benefits

The advantages is useful to obtain:

1) The optimum condition of bioactive in *M. elengi* Linn. leaf extract as natural product to synthesis the metal nanoparticle.
2) The potential of antioxidant and cytotoxicity from green synthesis silver and zinc oxide nanoparticles produced from *M. elengi*.

CHAPTER 2
LITERATURE REVIEW

2.1 *Mimusops elengi* Linn.

2.1.1 *M. elengi* botanical background

Mimusops elengi Linn. (*M. elengi*) is a tree that has a height approximately 20 meters. The bark is thick, hard and heavy. The trunk is straight with spreading branches. The leaf is green, thick, small, oval and wavy at border. The flower white, fragrant, the size about 2.5 cm, the shape of buds is ovoid, length of pedicels about 6.20 mm (Baliga et al., 2011).

This plant has variety of common name. In English called Bullet wood, in Thailand called Bakul or Pikul, in Indonesia called Tanjung (Gami et al., 2012). *M. elengi* plant can be found around Thailand, especially in Pattani Province. These are the picture of tree and leaf of *M. elengi* at **Figure 1.** as bellow.

(a) (b)

Figure. 1. (a) Tree and (b) leaf of *Mimusops elengi* Linn.

2.1.2 *Mimusops elengi* L biological activity

M. elengi has various pharmacological properties such as antibacterial, anti-fungal, antioxidant, anti-cariogenic, anti-diabetic and antineoplastic, gastro protective and diuretic. Antioxidant effects of methanolic extract from *M. elengi* leaf effective in some assay such as DPPH (Diphenyl Picrylhydrazyl Assay), *in vitro* reducing power assays and other total antioxidant

assay. Research by Baliga (2011), about chemical and biological properties of *Mimusops elengi* Linn had result that the various fraction of soluble phenolic esters, insoluble phenolic acid esters and free phenolic acids have free radical scavenging activities in DPPH and ABTS (2,2'-azino-bis (3-ethylbenzothiazoline-6-sulphonic acid) assays.

The extract of *M. elengi* bark has high value of total phenolic compounds which adequate for inhibiting radical to terminate the chain reaction. Phenolic compound of this extract plant has strong antioxidant potential activity by preventing DPPH and ABTS radical scavenging activity. It also takes a role as reducing agents (Rao et al, 2011). Research by Prakash et al. (2013) revealed that *M. elengi* leaf extract has potential as green reducing and stabilizing agent for synthesis silvernanoparticles (AgNP) by green synthesis method. The formation of AgNP ensured by UV-Vis spectroscopy. The AgNP are crystalline and stable confirmed by XRD pattern. SEM studies showed that AgNP were spherical shape in the range 55-83 nm. This green synthesis is conventional method but most rapid and eco-friendly than physical or chemical synthesis.

The *M. elengi* extract served as reducing and stabilizing agent which ensured by FTIR studies. For TEM and XRD studies showed that the synthesized AgNP were crystalline which the particle size around 23.5 nm. The AgNP has antioxidant activities which stable or can be used for more than 5 months. Biosynthesis method is preferable among chemical and physical method, because it has potential in medical and technological applications and also can be extended in large scale production (Kumar et al., 2014). Research by Natungnuy and Poeaim (2018) showed that *M. elengi* flowers has phenolic compound and provided antioxidant activity for DPPH, ABTS and FRAP assays. Methanolic extract of this plant revealed high antioxidant and cytotoxicity activity.

2.2 Nanoparticle

2.2.1 Nanotechnology

Nanotechnology has become important and exciting fields in science and technology. Nano in the word nanotechnology means the size of particle in a billionth (1×10^{-9}) meter. (Poole et al., 2003). Nanotechnology is system that can improve the structures and components in physical, biological and chemical properties because the particle in nanometer size. Nanotechnology is the developing technology to make very small particle, in nanometer scale approximately about 1-100 nm. The creation of structures and system can make new properties because the ability to be controlled on the small size or in atomic scale (Lane, 2000). Nanotechnology is engineering with atomic precision.

Many organisms such us plants, microbes and invertebrates are the source of natural products. Natural products have some biological activities as antibacterial, antifungal, antiviral and cytotoxicity which possess a large potential therapeutic effect. Plants have been the basis of traditional medicine in existence for thousands of years. Plant contributes around 25% of all the drugs in natural products and their derivatives for clinical use. Mostly the tropical world's flowering plant species which has potential as drug species. Isolation of bioactive compound can be obtained from the plant which collected separately from stem, root, root bark, bark, wood, leaf, and flowers. Quick drying of the part of plants is important to prevent degradation of the compound by microbes or air. The material has to dry to make constant weight, and then make it became smaller particle by grounding. Isolate of bioactive compound can be obtained by extraction using appropriate solvent. The major extraction techniques to get most bioactive compound is cold extraction called maceration. Aqueous extract stored at -20 °C to decrease the degradation. Crude extract can be used for bioassay method.

The metabolic performance of natural products can be separated into two groups, primary and secondary metabolism. Primary metabolites connect to fundamental process in all plants such as photosynthesis, glycolysis, etc. It produced and converted to molecular unity to create, preserve and reproduce the living cell of organism. Primary and secondary metabolisms are interconnected

which secondary metabolites can be flash back from primary metabolites. On the other hand, secondary metabolite is the derivatives of primary metabolites. Secondary metabolites have been known as biochemical differentiation. It represents a huge source to develop innovative drug. It can be classified by their chemical structure. Phenol and phenolic glycosides are one of the largest groups of secondary metabolites. There are phenolic classes of pharmaceutical interest such as simple phenolic, tannins, coumarins, quinones, flavonoids, lignans, terpenoids and steroids.

Bioassay is the most of significant phase for analysing the phytochemical activity of plants extract. In the beginning stage, *in vitro* testing has preference than *in vivo* studies that used animals as laboratory models. *In vitro* testing is preferable based on ethical, scientific and economic ground. *In vivo* testing is being used at stage of the experiment which based on the nature evident and the amount of the existence of bioactivity from *in vitro* testing (Havlicek and Spizek, 2014).

The properties of nano materials involved physical, magnetic, thermal, mechanical, chemical, optical and electronic properties. Physical properties examined about increasing the number of atoms in the surface that affect to nanomaterial's action such as quantum size effect, ultra-high surface effect, and ultrahigh volume effect. Magnetic property is about the presence of external magnetic force. The state of electron pairing in materials can be divided into paramagnetic and diamagnetic. Thermal properties are about the changes of particles size of materials that affect to thermal conductivity, lattice waves and interactions between nano materials. Mechanical properties are about the strength and elasticity of materials that can be created by decoration, modification and purification of microstructural scale. Chemical properties are about ionization energy that related to electron affinity. The increasing of surface area can increase the rate of reaction, efficacy and selectivity of chemical reaction. Electronic properties are about the changes of dimension affect to electronic structure because of the energy changes on the valence band between HOMO and LUMO conduction

bond. Atom has positive charge nucleus that surrounding with electron. Nuclei provide electrostatic attraction to electron rather than gravity.

There are some applications of nanomaterial such as nano catalysis, sensor and actuators, photovoltaic cell, fuel cells, battery and biomedical applications. Biomedical applications involved novel nano drug delivery system (NNDS) and nano cancer imaging (NCI). The NNDS is about the effectiveness delivery system in rate and time reaction. The NC is about the attractiveness of nanocrystal as probes for biomedical system. It preferable to use because can increase sensitivity, enhanced contrast and high precision. Nanomaterial have been designed with multiple vectors for attacking cancer cells at cellular level which higher precision and less side effect. Diagnosis of cancer can used vary of nanomaterial, such as nanostructured metals, transition metal oxides and metal organic complex (Liu and Bashir, 2015).

2.2.2 Green synthesis of nanoparticles

There are many methods such as biological, chemical and physical synthetic methods have been used to produce nanoparticles. Biological or green method is production the metal nanoparticles by natural source like plants, it is steadier than used other organisms. Plants are better to reduce metal ions rapidly compare to the other organism like bacteria or fungi. Plant extracts are preferring to use than plant biomass. Many biomolecules in plants have role in bio reduction, stabilization and formation of metal nanoparticle. The presences of polyphenols and enzymes in plants can affect the nanoparticle production (Iravani, 2011).

Physical synthesis is very expensive and also getting less amount of yield. On the other hand, chemical synthesis methods are harmful and contaminate the environment. Chemical synthesis is consuming cost and time. Thus, green synthesis is eco-friendly and low-cost. In green synthesis can used bacteria, fungi and plant. Synthesis of NP using extract of plant is more effective for getting more yield than using microbial, because it has some metabolites such as polyphenols that take a role as reducing and stabilizing agent in the biosynthesis of NP. It is eco-

friendly (used nontoxic chemicals), economic and more stable than using microbes and fungus.

Purification of nanoparticle (NP) is needed before attaching them in any applications. Centrifugation has been used to purify the nanoparticles because need few times consuming. High speed centrifugation and repetitive washing has been applied to separate and purifying the unreacted bioactive molecules. This method has limitedness such as it may cause agglutination of NP, changing the property of the NP and destabilization of NP.

The variation of pH, temperature and reaction time affect to morphology (shape and size), rate of synthesis of the NP and chemical properties by controlling the establishment of nucleation centers. The various shapes (spherical, rod like, triangle, octahedral platelets), size and reaction rate of synthesis of NP are dependent on temperature. The increasing of temperature affects to the increasing of reaction rate and formation of nucleation center. The sizes of the NP were more consistent and spherical in shape at higher temperature (50–60 °C). The decreasing of NP size occurred because of the increasing temperature but getting more yield. The pH of NP also related with the formation of nucleation center. The increasing of pH affects to the increasing of number of nucleation centers and raising the formation of metallic NP. The pH of NP affects to morphology and size of the NP. The number of NP was formed at lower pH but the size of the NP became larger. Aggregation forming larger sized NP because NP do not form more nucleation centers. Aspect ratio and size decreases with increasing pH. Reaction time similar with the pH and temperature, they affect to the morphology of NP. The increasing reaction time, make the increasing of particle size because of aggregation of particles (Singh et al, 2020).

Synthesis of metallic nanoparticles can use polyphenol as solvent, reducing, complexion and stabilizing agents. Liquid phase synthesis using polyphenol group to react with metal salts with different portion by heating the solution. Centrifugation has function to separate the particles from the liquid then being washed using ethanol. The dried particles being kept for further use.

Medicinal plants give more advantages and it simple for advance the nanoparticles into large scale production of. Green synthesis method using the part of plant such as leaf, flower, fruit, root, bark, stem etc. which being combined with aimed metal salt solution such as Zinc acetate (Zn (CH_3COO) $\cdot 2H_2O$), Silver nitrate ($AgNO_3$), and other metals.

The change of color examined to confirm the formation of nanoparticles. Many techniques being used for characterization of synthesized nanoparticle. X-ray diffraction (XRD) analysis is revealed the average crystallite size of nanocrystals. The optimum absorbance of the synthesized nanoparticle was determined by Fourier transform infra-red (FTIR) spectroscopy and UV–Vis spectrometry, they use to analyze the functional groups implicated. The shapes were analyzed using transmission electron microscopy (TEM).

The nanoparticles reveal the cytotoxicity activity by inducing cell cycle arrest or apoptosis. The nanoparticles in smaller size get into the cancerous cells by nucleus and it caused DNA damage which leading cell death. The cytotoxicity effects of nanoparticles occurred because the generation of reactive oxygen species which interference of thioredoxin and glutathione system.

The nanotechnology well known as the most promote for cancer therapy. The nanoparticle has revealed some potential to cure some type of cancers. The synthesized nanoparticles that using medicinal plants are non-toxic, they are fit in therapeutics and medical sciences. The potential of nanotechnology can increase the efficiency of drug targeting and decrease drug toxicity (Chandra et al., 2020).

2.2.3 Synthesis of silver nanoparticles (AgNP)

The AgNP can be synthesized in various shapes such as rod, spherical, flower-like, triangle, octagonal, hexagonal, etc. Smaller size particles which have larger surface area can cause more toxicity. Shape is also fundamental to the forming of toxicity. The AgNP toxicity consider to the presence of biological layer on the nanoparticle surface. The surface charges can establish the toxicity effect in cells. The positive surface charge of AgNP caused them more appropriate,

allowing them to match for a long time in blood stream contrast to negatively-charged NP, which is indicate as anticancer agents.

The molecular mechanism of AgNP revealed that cell death was depend on concentration under conditions. The AgNP can induce apoptosis and sensitize cancer cells. It induced the change in cell morphology, decreasing metabolic activity and cell viability which increased oxidative stress heading to increased production of reactive oxygen species (ROS) and mitochondrial damage, ending with DNA breakdown. The AgNP treated cells prevented many deviations, including down regulation of major actin binding protein, filamin, and mitotic arrest and up regulation of metallothionein.

The AgNP were capable of soaking up cytosolic proteins on their surface affect to the function of intracellular factors, and can set gene expression and pro-inflammatory cytokines which can change the regulation of more than 1000 genes. The possibility of using AgNP anticancer medical agent because of the normal side effects of radiation and chemotherapy. Although AgNP play an fundamental role in clinical research, many factors need to be inspected, including the method of production, the source of raw materials, bio-distribution, stability, controlled release, cell-specific targeting, accumulation, and finally toxicological effect to human beings. Then, to ensure the biosafety of the use of AgNP in humans, have to do research conducting about biocompatibility of AgNP and their associate with tissues and cells. It has to give a viable, reliable, and safe treatment of diseases with advance accuracy (Zhang et al., 2016).

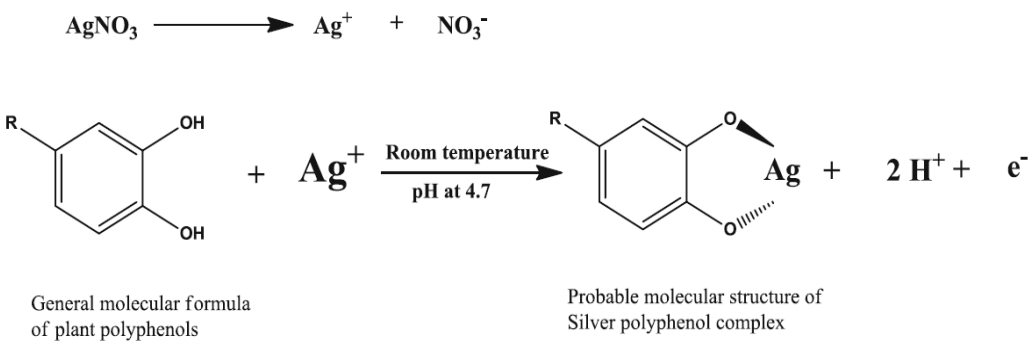

Figure 2. Green synthesis of silver nanoparticle

Source: Annavaram et al. (2015)

Research by Annavaram et al. (2015), about green synthesis using *Limonia acidissima* leaf extract to produce silver nanoparticles showed that the method is eco-friendly, efficient and simple route for synthesis of nanoparticles. The FTIR result proved that AgNP can be stabilized because the interaction of polyphenols, amines, carboxylic acids, alcohols and ketones. The TEM and XRD images confirmed that the stabilized AgNP were about 20–40 nm with which have a spherical shape with size of 30 nm.

Research by Prakash et al. (2013), about synthesis of silver nanoparticles (AgNP) from *Mimusops elengi* L. leaf extract have the result that for formation of stable AgNP have spherical shape of particles with radius about 55-83 nm. The reduction of Ag^+ ion with the presence of functional group, especially polyphenol in the leaf extract of *M. elengi* L, as the reaction at **Fig. 2**. It can be determined using FTIR. The nanoparticle formation was assured using the surface plasmon resonance band with UV–Vis spectrophotometer. The morphology and topography of the particles were revealed using SEM. The nanoparticles crystallinity was ensured with XRD pattern.

The synthesized AgNP using *M. elengi* can be noticed through the change of solution color from yellow to reddish brown and revealed by surface plasmonic resonance (SPR) band at 429 nm, which determine with UV–Visible spectrophotometry. Morphology and size of AgNP can be measured by TEM analysis. The XRD analysis showed the crystallinity of AgNP. The stability of AgNP was because of oxidizing polyphenols which can be revealed by FTIR analysis. Analyses of sample extracts when before and after reduction were executed, in order to determine the polyphenols in reducing Ag^+ ions to AgNP. The synthesized AgNP has application as antibacterial and antioxidant activities (Kumar et al., 2014).

2.2.4 Synthesis of zinc oxide nanoparticles (ZnONP)

Biologically synthesized ZnONP have application as drug delivery and anticancer therapy. The biocompatibility of ZnONP with no significant toxicity by in vivo and also in vitro. For evaluating the proliferation of some cancerous cells, the cytotoxic were performed by MTT assay. The greater in vitro inhibition of cancerous cell proliferation occurred at higher concentration and less effect on target cancer cells at lower concentrations. The varying sized nanoparticles simplify the drug target and showed a suitable agent to improve the drug delivery for cancerous cells. It has ability to kill the cancerous cell as drug delivery vehicle (Ahmed et al., 2017).

Phytochemical content in the T. *castanifolia* leaf extract have the important role in biogenic formation of ZnONP and also for the antioxidant, antibacterial and anticancer activities. The ZnONP has application for releasing the nano size drugs into targeted site in the body (Sharmila et al., 2019). The other research by Sonane et al. (2017), revealed that curcumin and vitamin C can repair the toxicity of ZnONP in C. *elegans*. The antioxidant was effective against nanoparticle toxicity and also resistance to other exposure. The use of antioxidants can role as an easy and economic method for minimalizing the nanoparticles toxicity.

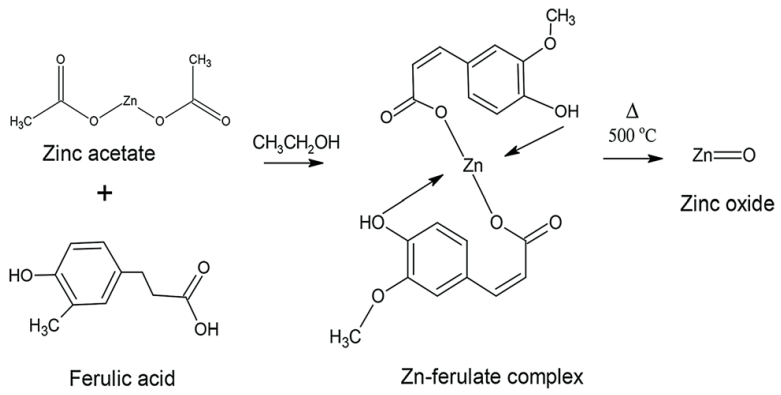

Figure 3. Green synthesis of zinc oxide nanoparticle
Source: Babu et al. (2015)

Synthesis of ZnONP using direct thermal decomposition method research by Das et al. (2013), have the result that the XRD pattern confirm the formation of quartzite and the particle size about 46.49 nm. The TEM and SEM result also revealed the ZnO nanoparticles formation. Antioxidant value of ZnONP was increased with concentration increasing. The nanoparticle showed the capacity of free radical scavenging that up to 91%. It has good antioxidant activity. Thus, this nanoparticle can be used as antioxidant in biological system.

The structures of ZnONP from extract of *Ricinus communis* can be determined by FTIR spectroscopy, FE-SEM/EDX and XRD. The powder of sample which being measured by FE-SEM and XRD gave results the formation of ZnONP crystallinity. The synthesized of ZnONP from *Ricinus communis* extract during the establishment can be revealed by FTIR spectra. Furthermore, the ZnONP can be applied as antioxidant, antibacterial and anticancer activity. The smaller size of NP, the higher potential as antibacterial, antioxidant and anticancer activity. The results of that activity depend on morphology and size. The smaller size of NP, the higher antioxidant and antibacterial activity. (Zare et al., 2018).

2.3 Characterization of silver nanoparticle (AgNP) and zinc oxide nanoparticle (ZnONP)

2.3.1 Characterization using UV-Visible Spectrophotometer

UV-Visible (UV-Vis) is spectroscopy based on absorption for measuring the beam light that have been absorb when its reflection of specimen or getting through specimen. It gives information of functional group, compound containing chromophore, conjugation of compound, quantitative and qualitative analysis. The spectra range for UV light from 200-400 nm, thus for visible light from 400-800 nm. The UV-Vis spectra can be produced when electrons absorb frequency (υ) transition from highest occupied to lowest unoccupied molecular orbital. When light get through the specimen, transition happen in the molecule, some part of light energy is infiltrate by the molecule when the energy of light similar with energy of electrons. UV-Vis spectrometer detects the distinct absorption wavelength and interpret data, wavelength versus absorbance in

nanometre scale. The UV-Vis can be used to analyse metal, metal oxide, organic compound and polymers.

On noble metal nanoparticles, such as AgNP, the character of plasmon was discovered to be transformed using different reducing agent. It also revealed that particle size highly affects to the width and position of the surface plasmon resonance (SPR). In the metal oxide nanoparticles, such as ZnONP, the absorption was unidentified, showing the full coating of ZnO core by phytochemical products (Liu and Bashir, 2015).

2.3.2 Characterization using Fourier Transform Infra-Red (FTIR)

Infra-red (IR) spectroscopy is method to determine the vibrational modes of a molecule. The IR spectroscopy can detect asymmetric vibrations of polar group. It also can reveal interaction between light and matter that make electric dipole mediated transition among vibrational energy level. The IR vibrational bands can be characterized by band shape (environment of bonds), frequency (energy) and intensity (polar character or polarizability). Every molecule has uniqueness of vibrational energy levels that called fingerprint of a particular molecule. The frequencies of molecular vibration based on some factor such as the strength of chemical bond, the geometric arrangement and masses of the atom. The functional group indicate characteristic vibration. Group frequency analysis can be used to show the presence and absence of various functional group in the molecule. (Larkin, 2011).

2.3.3 Characterization using X-Ray Diffraction (XRD)

X-Ray diffraction is rapid, non-destructive technic to determine the crystalline structure of multicomponent mixture such as nanomaterial, also to identify sample purity, atomic spacing and unit cell structure without extensive sample preparation. Monochromatic X-rays produce from cathode ray tube by heating the tungsten electron. Diffraction ray or constructive interference is making when x-ray contact with specimen, this can be revealed with Bragg's Law ($n\lambda=2\sin\theta$) which correlates with wavelength of electromagnetic rays, lattice

spacing and diffraction angle. All proper diffraction leading of lattice structure are getting into a range of 2θ angle in the distribution of powder particles. Each material has its own d-spacing; material can be determined by modifying diffraction peaks to d-spacing. XRD analysis being used in many fields such as mineralogy, metallurgy, archaeology, condensed matter physic, forensic science, biological and pharmaceutical sciences. The result of this method revealed on crystallinity, phase identification, lattice parameter and physical strength.

Green chemistry to produce silver nanoparticle which silver as noble metal revealed that with the increasing concentration of reducing agent affect to the decreasing of crystalline size of nanoparticles. The fabrications of nano metal have impact to highly reproducible various XRD spectra. Transitional metal oxides such as ZnONP have high photo catalytic and tuneable magnetism. Nano metal oxide has been made to control particle size and distribution. It also to exhibit low toxicity, biodegradable, biocompatible and controllable surface area (Liu and Bashir, 2015).

2.3.4 Characterization using Transmission Electron Microscope (TEM)

In the TEM system, electrons beam is transmitted over a specimen. There are interactions between the crystalline materials with electron beam by diffraction. TEM is the best instrument to characterize nanomaterials. The high energy of electron beam through thin layer of sample. The property of material such as structure, boundaries and dislocation showed over TEM by intercommunication of electron and atoms. The size, shape, thickness of well and quality of nano materials can be determined by the high-resolution electron beam of TEM. Electron being used instead of light to exploit the structure of nano materials. The wavelength of electron (2.43×10^{-12} m) is smaller than the wavelength of light, therefore image that showed from TEM is higher magnitude. Characterization of crystal dimension can be fast and accurate. High contrast, high spatial resolution, range of analytical capabilities and unsurpassed versatility which indicate TEM is the best technology for analysing nanoscopic specimens. The TEM have implementation in the fields of biology and life science, pharmaceutical quality

control, material research, defect analysis and high-resolution imaging.

Synthesis of silver nanoparticles which silver as noble metal, under green synthetic route can obtain the morphology, shape, size, chemical and thermal stability thus this factor affects to physicochemical, magnetic and optical of nano materials. Transitional metal oxide, such as ZnO can enhance super paramagnetic at nanoscale, which increasing local temperature. This mechanism can be applied for destroying the cancer cell (Liu and Bashir, 2015)

2.4 Application of silver nanoparticle (AgNP) and zinc oxide nanoparticle (ZnONP)

2.4.1 Antioxidant activity

The main oxidation of phenolic antioxidants is free radical scavenging, although flavonoids can also chelate metal ions. As antioxidants, phenolic compound donate hydrogen to peroxy radicals resulting in phenolic radicals. It can react with peroxy radicals form phenolic peroxy species which tend to degradation. Phenolic compounds can be oxidized by single oxygen. Flavonoid represents a wide range of secondary plant phenolic containing the flavan nucleus. These compounds are commonly found in the leaf, seeds, bark and flower. Flavonoids can be classified into flavonols (quercetin), flavones (luteloin), isoflavones (genistein), flavanones (naringenin), flavanons (epigallocatechin) and anthocyanidins (cyanidin) The protective effect of flavonoids in biological systems are strengthen by antioxidant capacity to terminate free radicals and inhibit oxidases.

There are many assays to determine the antioxidant activity. The assays related with radical scavenging, including the 2,2-diphenyl-1-picrylhydrazyl (DPPH) assay, the ferric reducing antioxidant power (FRAP) assay and the 2,2’-azino-bis(3-ethylbenzothiazoline-6 sulfonic acid) (ABTS) assay. At least have to used three different assays for determining the antioxidant activity. Measuring the product formed by oxidation using a spectrophotometer is a fast method to establish the antioxidant activity of the chemicals (Bartosz, 2013).

M. elengi is the medicinal plant to treat many diseases. The research by Gadamsetty et al. (2013), about in vitro antioxidant of leaf extract revealed higher free radical scavenging activity compared to standards with IC_{50} of 10.25 µg/mL (DPPH) and 13.5 µg/mL (ABTS). The results indicate that *M. elengi* leaf show good anti-oxidant properties. The phenolic, flavonoids are important role as antioxidant. Research by Rao et al., 2011, about antioxidant potential of *Mimusops elengi* bark that have result that IC_{50} values in DPPH radical, hydroxyl radical and ABTS radical were about 2.43 µg/mL, 152.76 µg/mL, 14.12 µg/mL and 6.31 µg/mL. Total phenolic content determination of *M. elengi* was using Folin–Ciocalteau reagent have contents about 375.9 mg/g, which greater than standard of gallic acid. The results revealed that *M. elengi* has potential as natural anti-oxidant.

2.4.2 Anticancer activity

Cancer can cause the death in humans which is estimated about 8.2 million and will increase to 13 million worldwide per year until years of 2030. Study about cancer became the greater therapeutic area consider of clinical trials and research and development and also the amount of project. The research about how to increase the effectiveness of anticancer drug being recommended. The greater level of ROS is important for viability of cancer cell, prolificacy of cell and metastasis by redox signaling regulation. The ROS are oxygen which having chemical species with great reactive properties and have contents superoxide anion, hydrogen radical and non-radical molecules for example is hydrogen peroxide. They were dangerous to cells because of they can react with other cell and harm to biomolecules, such as nucleic acids, proteins, and lipids. The ROS play a role as second messengers of signaling transduction in cell stress responses and cellular physiology. It also can set multiple cancer related signaling pathways by the modifications of reversible oxidative post translational (Xu and Mao, 2016).

The development of cancer drugs has guide to find new drugs that are toxic to the cancer cells but having not dangerous effect on normal cells. Currently, the research of anticancer drugs is being conducted with plants. The cost

of extraction of these substances from natural product is cheaper than the cost of the chemical synthesis (Lichota and Gwozdzinski., 2018).

The previous decade research advance in cytotoxicity against colon cancer. Family history was common for colon cancer risk factor. The symptoms of colon cancer have been determined and the testing of clinical genetic. The validation of big risk screening and the development to improve the screening tests will be needed for the future research (Burt, 2000). Research by Sahu (2016) showed that 20-50 nm nano silver was interact with Caco-2 cells to induce cellular toxicogenic responses. The cellular pathways influenced by the nano silver exposure can guide the increasing of toxicity. This study has result that toxicogenic characterization of human Caco-2 cells is an in vitro tool for nanoparticles assessing toxicities (Sahu, 2016)

2.4.3 Mechanism of toxicity in silver nanoparticle

The toxicity of nano silver is related to the change in environmental and biological media such as interaction with biological macromolecules, release of silver ions and surface oxidation. Nano silver particles can react with membrane of proteins and signaling pathways being activated, guide to inhibit cell prolificacy. The nano silver particles can go through the cell by endocytosis or diffusion to lead generation of reactive oxygen species (ROS), mitochondrial dysfunction, leading to harm the proteins and nucleic acids inside the cell, and finally inhibition of cell proliferation. Oxidative stress occurs when the generation of ROS exceeds the capacity of the cellular antioxidant defense system. Depletion of glutathione and protein-bound sulfhydryl groups and changes in the activity of various antioxidant enzymes have been affected in oxidative damage. An important toxicity mechanism for nano silver is the interaction of both the ionic and nano form of silver with sulfur containing macromolecules such as proteins, due to the strong affinity of silver for sulfur (McShan et al., 2014).

2.4.4 Mechanism of toxicity in zinc oxide nanoparticle

The ZnONP are getting into the cell through endocytosis. The NP insert the cell, whereas some insert through phagocytosis and pinocytosis bounded by lysosomes and endosomes. The decreasing of pH affects to the increasing of the ZnONP dispersion rate, leading destabilization of lysosome. The pH 6.3 of endosome is low, which favors the loosed of soluble zinc ions. It decreases furtherly to pH 5.5 at late endosome and pH 4.7 in lysosome, where a fast dissolution rate of ZnONP and leading destabilization of lysosome. The low pH is necessary for losing the zinc ions in extracellular fluid or blood, that has a normal pH at 7, is not profitable. This process leads to increase the releasing of soluble zinc ions inside the cell which resulting in cytotoxicity. The increasing soluble zinc ions affect to the increasing of reactive oxidation species concentration, heading to cytotoxicity through oxidative stress (Bisht and Rayamajhi, 2016).

CHAPTER 3
METHODOLOGY

3.1 Overall Scope

The research scope of this work was summarized in **Fig. 4**

Figure 4. Flow chart of experiment

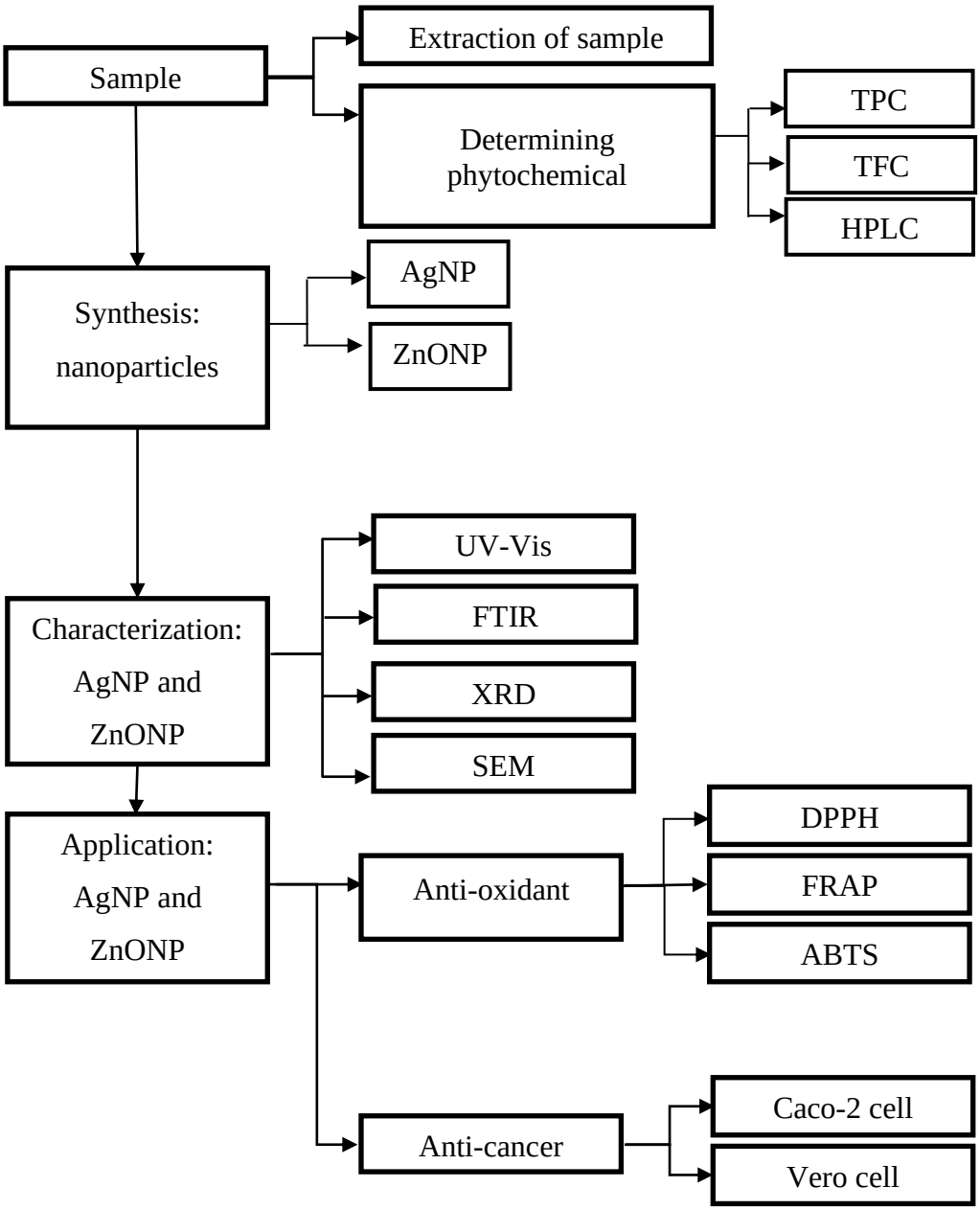

3.1.1 Chemicals and reagents

All chemicals and reagents are shown in **Table 1.**

Table 1. Chemicals and reagents

Reagent	Grade	Company	Country
Gallic acid ($C_6H_2(OH)_3COOH$)	Analytical Reagent	Sigma Aldrich	USA
Deionize water (H_2O)	Analytical Reagent	Merck	Germany
Phosphoric acid (H_3PO_4)	Analytical Reagent	Fisher Scientific	UK
Sodium nitrite ($NaNO_2$)	Analytical Reagent	Ajax Finechem	Australia
Aluminum chloride ($AlCl_3$)	Analytical Reagent	Ajax Finechem	Australia
Sodium hydroxide (NaOH)	Analytical Reagent	LOBA Chemie	India
Catechin ($C_{15}H_{14}O_6$)	Analytical Reagent	Sigma Aldrich	USA
Dimethyl Sulfoxide (DMSO)	Analytical Reagent	Fisher Scientific	UK
Folin-ciocalteu reagent (C_6H_6O)	Analytical Reagent	Sigma Aldrich	USA
Sodium carbonate (Na_2CO_3)	Analytical Reagent	Ajax Finechem	Australia
2,2-diphenyl-1-picrylhydrazyl (DPPH)	Analytical Reagent	Sigma Aldrich	USA
Ferric tripyridyl triazine complex (Fe^{3+}-TPTZ)	Analytical Reagent	Sigma Aldrich	USA
Silver nitrate ($AgNO_3$)	Analytical Reagent	Fluka Chemica	Switzerland
Zinc acetate (Zn $(CH_3COO)_2.2H_2O$)	Analytical Reagent	Ajax Finechem	Australia
Sodium Acetate hydrated ($CH_3COONa.3H_2O$	Analytical Reagent	Ajax Finechem	Australia
Iron (III) Chloride hexahydrate ($FeCl_3.6H_2O$)	Analytical Reagent	Chem Supply	Australia
Potassium Persulfate ($K_2S_2O_8$)	Analytical Reagent	Ajax Finechem	Australia
Ferrous Sulphate heptahydrate ($FeSO_4.7H_2O_)$	Analytical Reagent	Okhla Industrial	India
Acetic Acid glacial (CH_3COOH)	Analytical Reagent	J.T Baker	Thailand
Hydrochloric Acid (HCl)	Analytical Reagent	Merck	Germany

Reagent	Grade	Company	Country
Ethanol	Analytical Reagent	QRec	Switzerland
Trolox (6-hydroxy-2,5,7,8 tetra methylchroman-2-carboxylic acid)	Analytical Reagent	Sigma Aldrich	USA
ABTS (2,2′-Azino-bis (3-ethyl benzothiazoline-6-sulfonic acid))	Analytical Reagent	Sigma Aldrich	USA
Potassium Bromide (KBr)	Analytical Reagent	Merck	Germany
DMEM (Dulbecco's Modified eagle Medium)	Analytical Reagent	Fisher Scientific	UK
Trypsin	Analytical Reagent	Sigma Aldrich	USA
PBS (Phosphate Buffer Saline)	Analytical Reagent	Fisher Scientific	UK
Tryptophan ((2S)-2-amino-3-(1H-indol-3-yl) propanoic acid)	Analytical Reagent	Sigma Aldrich	USA
MTT (Thiazolyl blue tetrazolium bromide)	Analytical Reagent	Sigma Aldrich	USA
Vero cell	Industrial Grade	Fisher Scientific	UK
Caco2 cell	Industrial Grade	Fisher Scientific	UK

3.1.2 Plant samples

M. elengi L. leaf were harvested at February- March 2019 on around Prince of Songkla University, Pattani Campus, Thailand.

3.1.3 Glasswares

General glasswares were used such as beaker, volumetric flask, test tube, dropper, vial, glass watch, glass funnel and stirring rod. All glassware by Pyrex company from Germany.

3.1.4 General apparatus

Apparatus and instruments used for this research are shown in **Table 2.**

Table 2. Apparatus and instruments

Apparatus	Brand	Country
Rotary evaporator	Heidolph	Germany
Hot plate stirrer	Daihan LabTech	Germany
Vortex mixer	Scientific Industries	Thailand
Centrifuge	Centurion	UK
Water bath	Memmert	Japan
Hot air oven	Memmert	Japan
UV-Visible Spectrophotometer (UV-Vis)	Biochrom Libra S22	UK
Fourier Transform Infra-Red Spectrophotometer (FTIR)	Bruker Tensor 37	USA
X-Ray Powder Diffractometer (XRD)	Mettler Toledo	Switzerland
Micropipette 100-1000 µL	Eppendorf	USA
Micropipette 20-200 µL	Mettler Toledo	Switzerland
Analytical Scale	Mettler Toledo	Switzerland
Muffle Furnace	Thermolyne	USA
pH meter	Mettler Toledo	Switzerland
Incubated shaker	Jeio Tech	Korea
Sonicator	NDI	USA
Miller	Retsch	Germany
Siever 250 µm	Endecotts	UK
Microplate reader	Biochrom EZ Read 400	UK
Motorized pipette controller	Blue Swan	Taiwan
Manual liquid handling	Eppendorf	USA
Microscope eclipse E100	Nikon	Japan
Biosafety cabinet	Labogene	Scandinavian
Cell culture CO_2 incubator	Mettler Toledo	Switzerland
Transmission Electron Microscope	Hitachi	Japan

3.2 Material and methods

3.2.1 Preparation of *M. elengi* leaf extract

M. elengi leaf were collected from Pattani Province, Thailand. The leaf was washed with deionized water to remove dust particles. Thereafter, the leaf was shade dried and grinded with disc mill for 20 min into powder. The 25 g of the dried powder was macerated with 125 mL deionized water for 24 h at room temperature. After filtering through

Whattman No.1, paper filtrate was evaporated with rotary evaporator at 70°C for 6 h to get the water crude extract (Hayouni et al., 2007).

3.2.2 Phytochemical analysis of *M. elengi* leaves extract

3.2.2.1 Total Phenolic Content (TPC)

Briefly, the crude extract solution (50 µL) was mixed with distilled water (200 µL) and 10 % Folin–Ciocalteu reagent (50 µL). The mixture was incubated for 6 min at room temperature. After incubation, 7% sodium carbonate **(**Na_2CO_3**)** solution (500 µL) and distilled water (400 µL) were added, and incubated once again for 15 min at 45°C. The absorbance was determined at 765 nm. Gallic acid will be used as a standard. Total phenolic content was express as milligrams of gallic acid equivalents **(**GAE**)** per gram of extract (Hayouni et al., 2007).

3.2.2.2 Total Flavonoid Content (TFC)

The extract (50 µL) and 5% $NaNO_2$ (60 µL) was mixed and incubated at RT for 5 min. Thereafter, 120 µL of 10% $AlCl_3$ was added and stood for 5 min of reaction. 1 mM NaOH (400 µL) and distilled water (600 µL) were added to make the reaction completed. The absorbance was determined at 510 nm. Catechin was used as a standard. Total flavonoid content was expressed as milligrams of catechin equivalents (CE) per gram of extract (Hayouni et al., 2007).

3.2.2.3 HPLC analysis

Phenolic compound in sample had been determined using a HPLC-DAD (High-Performance Liquid Chromatography with Diode-Array Detection) system by comparing with phenolic compound standard. The HPLC apparatus used Phenomenex ODS (4.6 x 250 mm, 5µm), and a UV-Vis detector monitored at different wavelength 254 nm for gallic acid and chlorogenic acid, at 270 nm for ellagic acid, at 280 nm for catechin and epicatechin, at 340 nm for ferulic acid and at 370 nm for myricetin, quercetin and kaempferol. The injection volume of the extract was 10 µL. The separation was carried out at room temperature on a C18 column (3.0 18.4 mm). The mobile phase contained phosphoric acid and acetonitrile with gradient of mobile phase (Kamal et al., 2015).

3.2.3 Synthesis of nanoparticles

3.2.3.1 Synthesis of silver nanoparticle

There was 1 mL of the 1000 ppm extract was dissolved in 10 mL of silver nitrate solution at varied concentrations (1-7 mM). In order to optimize the best condition for the nanoparticle synthesis, the solutions were incubated by stirring at 400 rpm for 30-120 min at 25-70 °C with pH 3-11. After colour of the solution changed to reddish, the solution was further evaporated at 70 °C for 1 h and heated by a hot air oven at 90 °C for 6 h until getting dark dried powder (Kumar et al., 2014).

3.2.3.2 Synthesis of zinc oxide nanoparticle

Zinc acetate dehydrates solution 0.1 M 10 mL mixed with 1mL of the extracts in a magnetic stirrer for 2 hours at 60 °C. After that, the solution was stand for 8 hours. The particles became apparated by centrifugation for 20 minutes at 6000 rpm. After that, the supernatant or concentrate extract washed out with distilled water followed by methanol. Then, sample extract being dry in a hot air oven at 80 °C for 24 hours. Finally, the crude was calcinated in furnace at 350°C for 3 hours (Wang et al., 2018).

3.2.4 Characterization of nanoparticles

3.2.4.1 UV-Vis Spectro analysis

The sample solution (extract and nanoparticles) 1.5 mL has been took and put into cuvette. UV–vis spectrophotometer has been recorded by scanning the sample solution in the range from 200-800 nm at room temperature. The blank solution was distilled water (Kumar et al., 2014).

3.2.4.2 FTIR analysis

The nanoparticles concentrate powder mixed with potassium bromide (KBr) powder. After that, that mixed powder was grinded and pressed became thin layer. The FTIR analysis determined in the range of 4000–280 cm^{-1} (Kumar et al, 2014).

3.2.4.3 XRD analysis

Concentrate extract of sample has been made to became a thin film by drop coating the nanoparticles sample into carbon coated copper. Thin film of nanoparticle measured at 40 kV, 20 mA using Cu-Kα radiation (λ = 1.5418 Å). The diffracted intensities have been recorded from 3°-50°, 2θ angles at a scan rate of 0.5 degree/minutes (Kumar et al., 2014).

3.2.4.4 TEM analysis

The nanoparticles sample solution has been took and put into carbon grid. Then has been stand for 5 minutes and it became dry. Then residual of the sample removed using blotting paper. The TEM image recorded at 40,000× magnifications with 20.00 kV (Kumar et al., 2014).

3.2.5 Determination of antioxidant activities

3.2.5.1 DPPH radical scavenging assay

Antioxidant activity of extract sample has been checked before and after synthesis nanoparticle. Trolox standard or extract solution in different concentration (7.8125 – 500 mg/L) about 450 µL mixed with methanolic solution of DPPH 0.2 mM about 900 µL. After that, it was incubated for 30 minutes at room temperature. Trolox used as a standard and 450 µL of distilled water has been added instead of Trolox for control. The absorbance determined at 515 nm using UV–Visible spectrophotometer (Ahmed et al., 2017).

3.2.5.2 ABTS assay

The ABTS solution with concentration 14 mM has been added with 4.9 mM potassium persulfate in ratio 1:1 and then incubated in the dark for 12–16 hours at room temperature to became stock ABTS 7 mM. Trolox standard or extract solution in different concentration (7.8125 – 500 mg/L) about 120 µL mixed with stock ABTS solution about 1000 µL and the mixture incubated for 10 minutes at room temperature. The absorbance has been determined at the wavelength of 734 nm. Trolox being used as a standard, and 450 µL of deionized water being added instead of Trolox for control (Ahmed et al., 2017).

3.2.5.3 Ferric-reducing antioxidant power (FRAP) assay

The FRAP reagent (300 mM acetate buffer, 10 mM TPTZ solution in 40 mM HCl, 20 mM $FeCl_3$ in ratio 10:1) incubated for 10 minutes at 37°C. The ferric sulfate ($FeSO_4$) used as a standard. Ferric sulfate standard or extract solution has been prepared in different concentration (100-800 mg/L). After that, 40 µL of each sample solution mixed with distilled water about 200 µL and FRAP reagent about 1,200 µL. Then, it has been kept at room temperature for 20 minutes. The absorbance determined at the wavelength of 593 nm (Ahmed et al., 2017).

3.2.6 Cytotoxicity test

Colon cancer cell, Caco-2 and normal cell Vero in culture medium DMEM (1.0×10^4 cells/well) cultured in 96-well plate and grown for 24 hours at incubator. The culture medium removed and replaced with metal nanoparticle solution, then dilute in culture medium DMEM or equal amount of DI water as control (7.8-250 µg/mL) on extract (7.8-2000 µg/mL) and grown for 24 hours at incubator. Then, 200 µL of 0.5 mg/mL MTT solution has been added into each well for 4 hours. After that the spent MTT solution being removed, 250 µL of DMSO put into dissolve formazan crystals. Formazan solution has been detected at 560 nm by subtract from background at 670 nm (Wang et al., 2019).

3.2.7 Statistical analysis

The independent test, one-way Analysis of Variance (ANOVA) and post-hoc analysis (Tukey test) were performed to compare mean different between concentration within group for extract and nanoparticles (AgNP and ZnONP). Thus, two-way Analysis of Variance (ANOVA) and post-hoc analysis (Tukey test) were performed to compare mean different between concentration in different group among of extract and nanoparticles (AgNP and ZnONP). All experiment was performed three times independently using triplicate measurement. The values are expressed as mean ± SD. Statistical significant accepted at a level of $p < 0.05$ using IBM SPSS Statistics 24 version (Sonia et al., 2017).

CHAPTER 4
RESULTS AND DISCUSSION

This experiment has been determined phytochemical especially phenolic compound in *M. elengi* leaf extract. This plant can be found at South East Asia, the tree of this plant was shown at **Fig. 5a**. The plant has many different names in each country, in English name called Bullet wood, in Thailand called Pikul and in Indonesia called Tanjung (Gami et al., 2012). There are many bioactive compounds in every part of this plant that have many uses such as traditional medicine plant. The leave contains organic compound such as alkaloids, flavonoids, tannins, terpenoids, steroids, glycosides and benzenoids. Major bioactive compounds that contained in this plant are phenolic and flavonoid. Both of them play the role as antioxidant (Baliga et al., 2011).

(a) (b) (c)

Figure 5. *M. elengi* Linn. plant: (a) a tree (b) a leaf (c) the *leaf*.

4.1 Preparation of sample

Based on the result at **Table 3**, the weight of extract sample is 1.14 gram from 150 gram of fresh leaf. The calculation give result that the yield of sample was 22.8 % from weight of dried powder. Research by Begum et al (2018) revealed that the yield of *M. elengi* leaf methanolic extracts were 25.21 %. The different polarity of solvent affect to different yield which got from extraction. It is because methanol less polar than water, so the phenolic and another non polar compound in plant can dissolve in methanol so it got higher yield. But in this research using water

as solvent, only phenolic and polar compound can be dissolved so the yield less than using methanol as solvent. The using of aqueous extract because based on green chemical principle which using safety or eco-friendly substances, since the yield both of them are quite similar or not too different (Hayouni et al, 2007). Even though there are only little amount of polar compound like phenolic and flavonoid in leaf of *M. elengi* which taken by water, but it prefers to use because it safer than using methanol or other chemical as solvent.

Table 3. Percent yield of *M. elengi* leaf

Sample	**weight of extract (g)**	**% yield**
N1	1.05	21.00
N2	1.13	22.60
N3	1.24	24.80
Result	1.14 ± 0.10	22.80 ± 1.91

4.2 Determination of phytochemical

Bioactive or phytochemical compound in sample plant, especially phenolic and flavonoid, can be determine with total phenolic content (TPC) and total flavonoid content (TFC). Determining phenolic compound in plant with TPC method need standard like gallic acid to calibrate and to calculate the amount of phenolic compound in sample (Rosa et al., 2019).

Based on **Table 4** can be knowing that phenolic content in sample was 266.58 ± 45.27 mg/g GAE and for flavonoid content is 151.13 ± 3.77 mg/g CE. Research by Gadamsetty et al. (2013) found that phenolic content in *M. elengi* leaf methanolic extract was 40.3 mg/g GAE and flavonoid was 52.7 mg/g QE. Thus, in this research get higher amount of phenolic and flavonoid contain than previous study using same plant. It is because using different solvent, water can take phenolic and flavonoid more pure than using methanol that also can took other compound that also has hydroxyl group (-OH).

The result also showed that in *M. elengi* leaf extract has higher phenolic content rather than flavonoid contain. So, in this plant, phenolic content is more dominant than flavonoid content. This plant only has few of flavonoid, twice time less than phenolic content.

Table 4. Phytochemical in *M. elengi* leaf

Sample	Phenolic content (mg/g GAE)	Flavonoid content (mg/g CE)
N1	297.87 ±11.06	147.00 ± 2.50
N2	287.20 ± 6.21	154.50 ± 2.50
N3	214.67 ± 8.05	152.00 ± 5.00
Result	266.58 ± 45.27	151.13 ± 3.77

The TPC and TFC result also can be showed as diagram to know the relation about increasing concentration and phytochemical content in sample. The increasing of sample concentration has the increasing of phenolic content too.

After analysis with HPLC-DAD for all samples, there are many chromatogram from all of them. From the chromatogram can be know the retention time for identification the compounds and peak area for each of them to determine the concentration of sample. Thus, can be known that there is gallic acid in sample to because the retention time of both standard and sample are same.

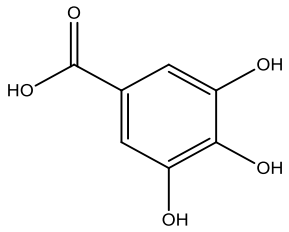

Figure 6. Chemical structure of gallic acid

4.3 Characterization of silver nanoparticles (AgNP)

The AgNP can be made from mixing the extract that contain phenolic and flavonoid compound with silver ion from silver nitrate. Phenolic and flavonoid that has hydroxyl group take a role as capping and reducing agent for Ag^{+} to become

Ag°. When the particle in nano size, it has larger surface area than the bulk or aggregate. Thus, the particle can be reacted effectively and efficiently.

There is some parameter that affect to synthesize AgNP, such as concentration of silver nitrate and extract sample, volume ratio that used for both of them, reaction time, temperature and pH (Sangaonkar and Pawar, 2018). All of that parameter can be varied to get optimum condition for synthesis the AgNP. Based on **Fig. 8** can be knowing that to get the best of AgNP followed this condition, 3 mM of silver nitrate about 10 mL combined with 5000 ppm of extract sample 1 mL, then synthesize using shaker at 200 rpm at 70 °C for 90 minutes under pH 11. Research by Kumar et al. (2014) showed that to synthesize AgNP using *Mimusops elengi* Linn. aqueous leaf extract needs 4 mM $AgNO_3$ and 5000 ppm extract with ratio extract:$AgNO_3$ (1:10) in alkaline condition (pH 9) because increase pH increase formation, it is occurred for 60 minutes at 90 °C, the nanometal formation when the colour of solution changed to reddish brown. Confirm by UV-Vis absorption spectra at 423 nm. Thus, the optimum conditions for synthesis AgNP using extract plant for this research was similar to previous research that also using plant that rich of phenolic and flavonoid compound even though in different plant. But the important factor is the phenolic and flavonoid content in plant.

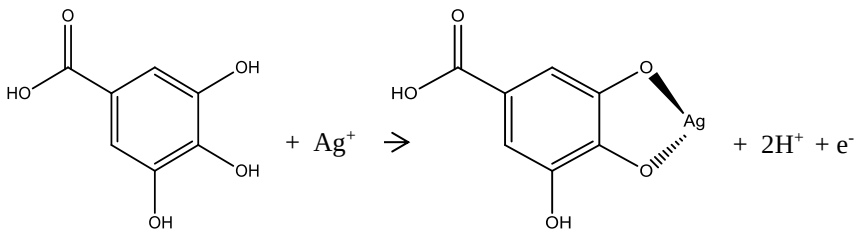

Figure 7. Synthesis mechanism of AgNP formation

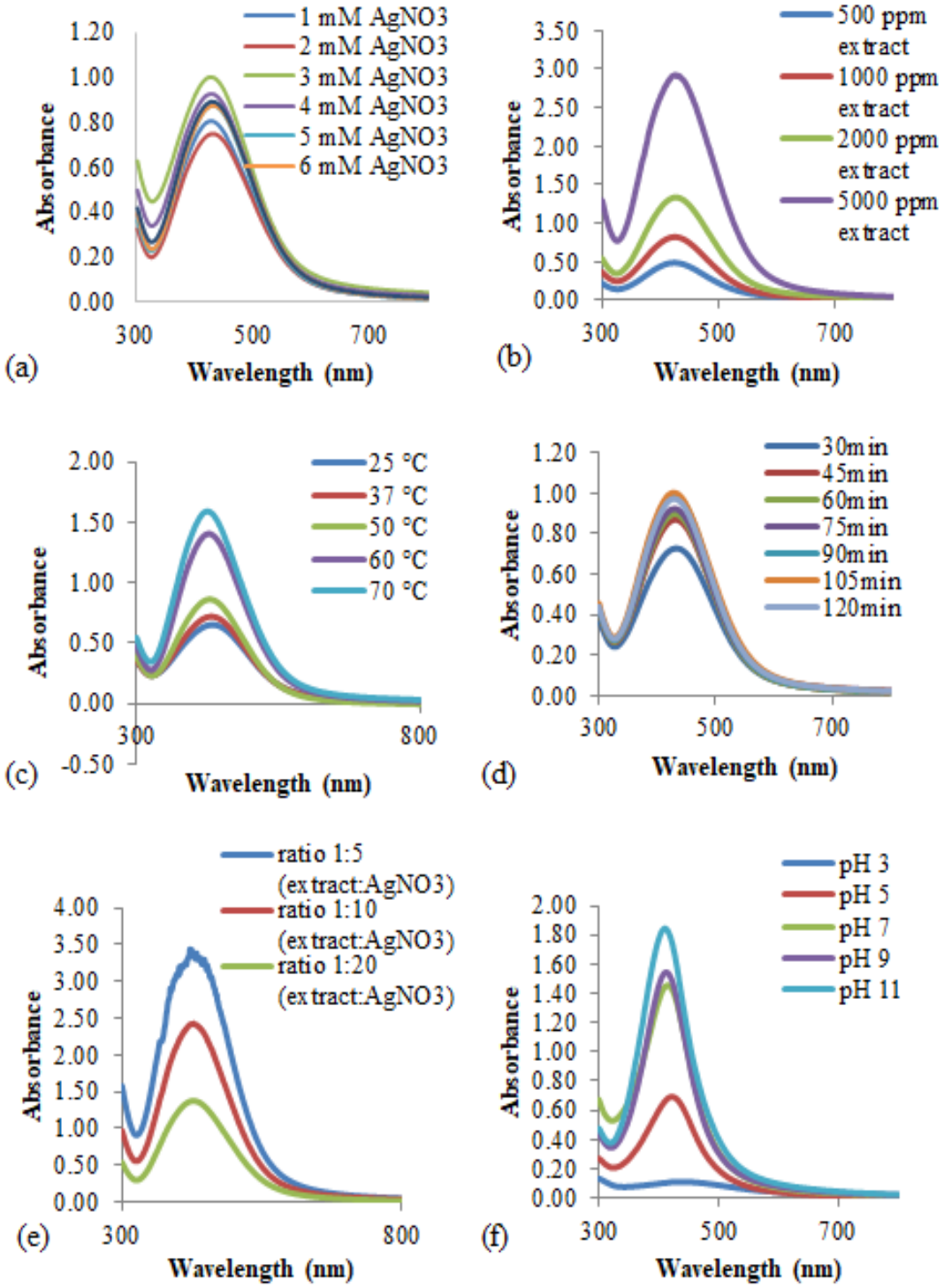

Figure 8. UV-Vis spectra of AgNP prepared by at different (a) concentration of $AgNO_3$ (b) concentration of aqueous *M. elengi* leaf extract (c) temperature (d) reaction time (e) ratio of extract and $AgNO_3$ (f) pH

The AgNP was firstly confirmed by UV-Vis spectrophotometer by determining the peak at around 420 nm that indicate the formation of AgNP. It also can be knowing by the colour changing of solution from yellow brownish to dark brown. The increasing concentration of silver nitrate and extract equals to the increasing absorbance. It is because higher concentration has higher silver ion and phenolic compound so there are many AgNP can be formed. The increasing reaction time also make increasing absorbance because the particle reacts with other in longer time so will produce more particle of AgNP than less reaction time. The increasing of temperature also make the increasing of absorbance because with heating the solution so the reaction rate can be faster than in lower temperature. The increasing pH also make increasing absorbance because in base condition or pH more than 7, there are many hydroxyl groups that can increase the AgNP formation.

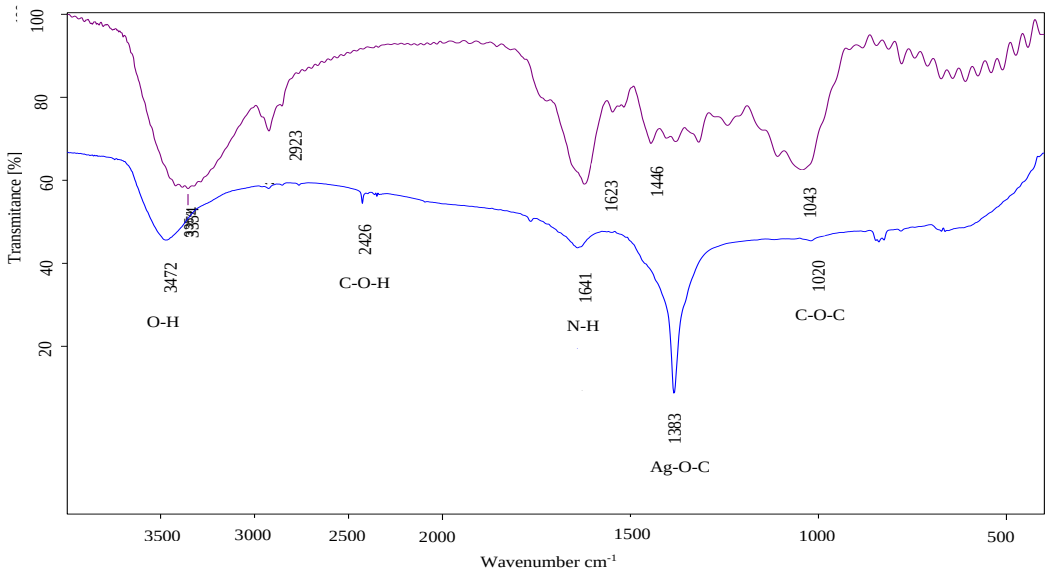

Figure 9. FTIR spectra of (a) *M. elengi* leaf (b) AgNP

Other characterization using FT-IR to know the changing particle structure of sample before and after synthesis. As shown in **Figure 9.**, AgNP displayed the band at 3354 cm^{-1} correspondence to O-H stretching of alcohol and phenol. The band at 2923 cm^{-1} correspondence to O-H stretch carboxylic acid. The band at 1623 cm^{-1} correspondence to N-H bend primary amines. The band at 1446 correspondence to C-O-H vibrations. The band at 1043 cm^{-1} correspondence to C-O-C

stretching. The FT-IR result of AgNP at figure 13, which the band at 3474 cm^{-1} correspondence to O-H stretching of alcohol and phenol. The band at 2426 cm^{-1} correspondence to alkyne bond. The band at 1643 cm^{-1} correspondence to N-H bend of amines. The band at 1446 correspondence to C-O-H vibrations. The band at 1383 cm^{-1} correspondence to C-O stretching in the spectrum of silver nanoparticle. The band at 1021 cm^{-1} correspondence to C-O-C stretching and compared both of them at **Fig. 9**

Research by Khalil et al. (2013) showed that to synthesize AgNP using *Olive* leaf extract, characterization using FTIR spectrum at 3385 cm^{-1} correspondence to O-H group of phenolic, and 1646 cm^{-1} correspondence to C=O of carbonyl, 1108 cm^{-1} correspondence to C-O of phenolic in extract and it was shift at AgNP into 3399 cm^{-1} correspondence to O-H group of phenolic and 1638 cm^{-1} correspondence to C=O of carbonyl and 1109 cm^{-1} correspondence to C-O of phenolic. The band at 2925 cm^{-1} correspondence to C-H of methylene group and the sharp band at 1383 cm^{-1} correspondence to Ag-O-C of AgNP. Thus, based on previous result compare to this research result, showed that the sharp band at 1383 cm^{-1} correspondence to Ag-O-C of AgNP. From that figure also can be know there are some shift of the peaks from higher to lower that indicate the AgNP formation. Because some functional group already bonding and capping the silver ion to make AgNP. So there was new chemical structure from AgNp which different with extract (Kumar et al., 2014).

Next step, the crystallinity of AgNP was further confirmed using powder XRD. Based on **Fig.10** showed the XRD pattern of AgNP that prepared using *M. elengi* leaf extract. There are some strong diffraction peaks at 2θ values of 38.2°, 44.5°, 64.5°, 77.5°, 81.5° which correspond to the (111), (200), (220), (311) and (222) interplanar reflections of face centre cubic (fcc) crystal structure.

Research by Khalil et al (2014) about synthesize AgNP using olive aqueous leaf extract, for characterization using XRD showed the Bragg reflection peaks at 2θ values of 38.25°, 44.30°, 64.39°, 77.35°, 81.37° that was indexed to (111), (200), (220), (311) and (222) planes of face centre cubic (fcc) structure of pure AgNP (JCPDS, File No01-087-0597). So after comparing the high peaks with other similar research and from standard that can be knew that the AgNP product from this research

also has face centre cubic (fcc) crystal structure. The intense reflection of (111) peaks compare to other peaks indicate the nano crystal (Ahmad and Sharma, 2012).

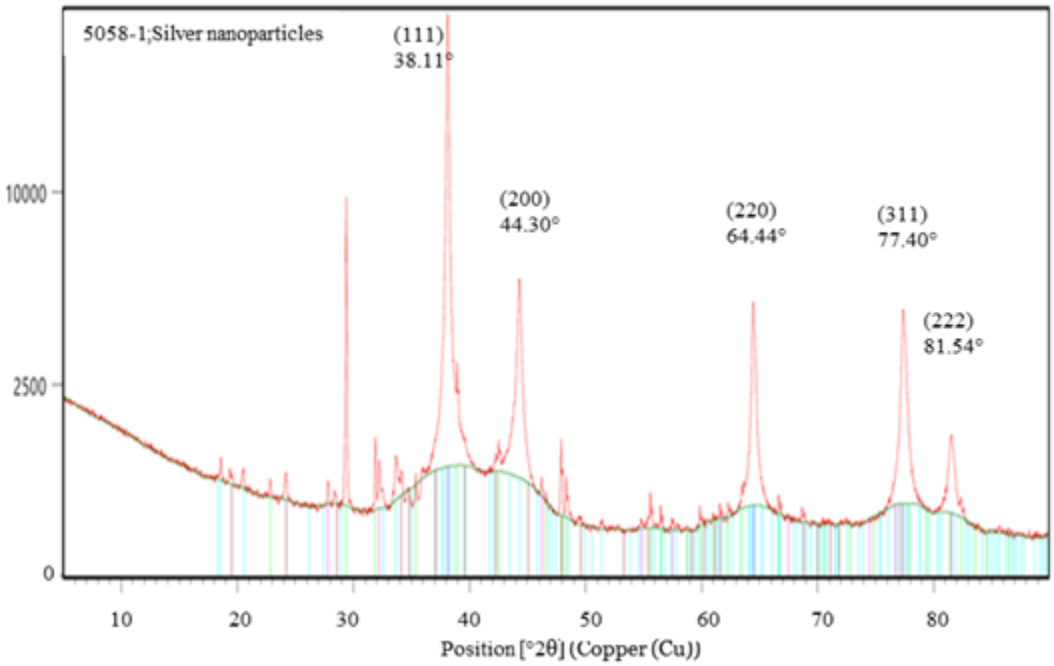

Figure 10. X-ray diffraction pattern of synthesized AgNP

Last step to confirm the nanoparticle of sample by using transmission electron microscopy. Based on **Fig. 11** revealed that the particle size of AgNP around 16.84 nm – 33.67 nm or the average of particle size around 22.12 nm. It can be confirmed that the AgNP already at the range of nano size particle (1-100 nm). Besides that, can be known that phenolic and flavonoid compound from extract, can coating the silver ion that have round and spherical shapes, like showed at **Fig. 11** (Khalil et al., 2013).

Research by Kumar et al. (2014) showed that to synthesize AgNP using *Mimusops elengi* Linn. aqueous leaf extract, for characterization using TEM revealed that AgNP was spherical shape with average particle size of 20 nm. The result both of them, previous and this research showed similar result that AgNP was spherical shape with average particle size of 20 nm. The particle size still in the range nano size (1-100 nm), so the AgNP result from this research already formed in nano size.

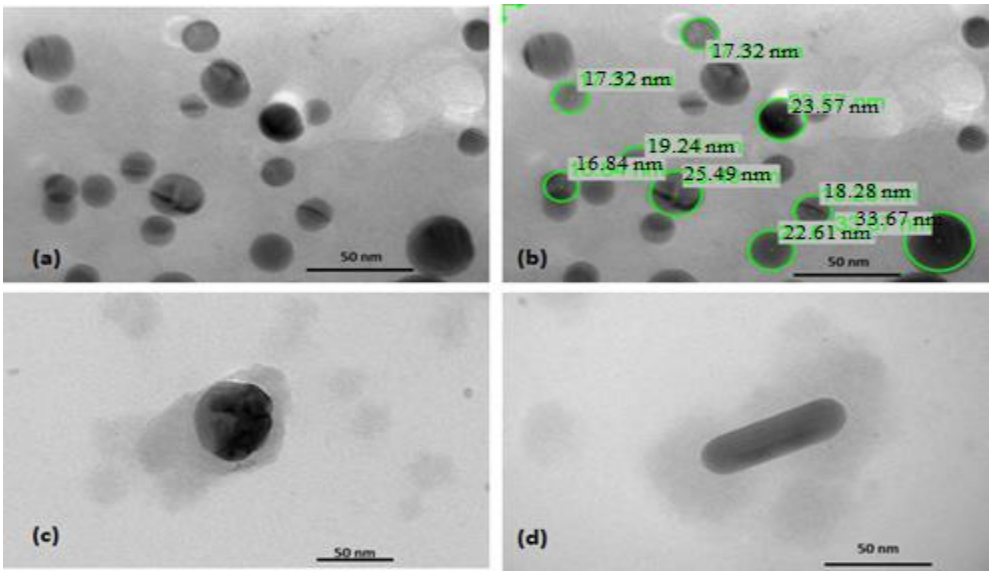

Figure 11. TEM images of AgNP (a) particles at 50 nm (b) particles size (c) spherical shapes (d) rod shapes

4.4 Characterization of Zinc oxide nanoparticles (ZnONP)

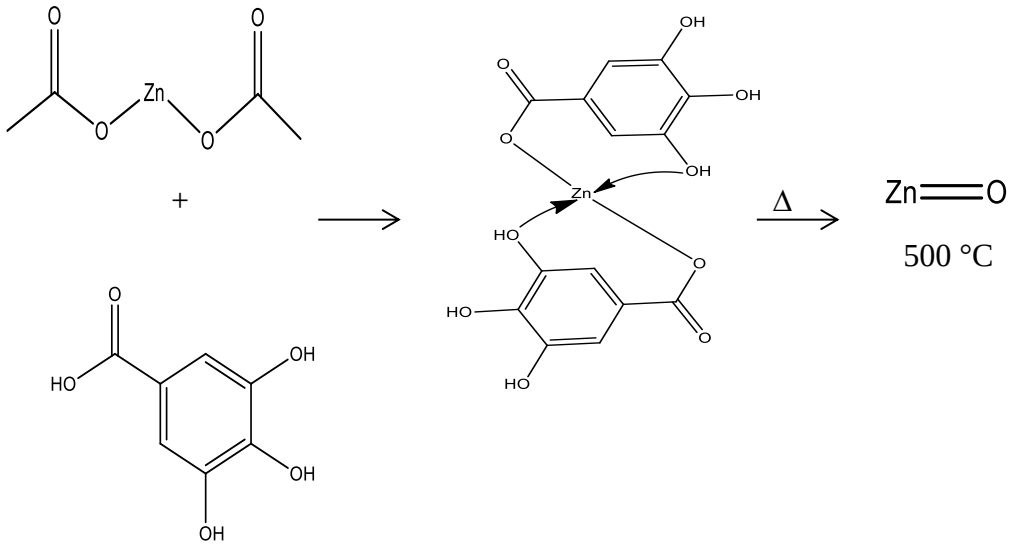

Figure 12. Synthesis mechanism of ZnONP formation

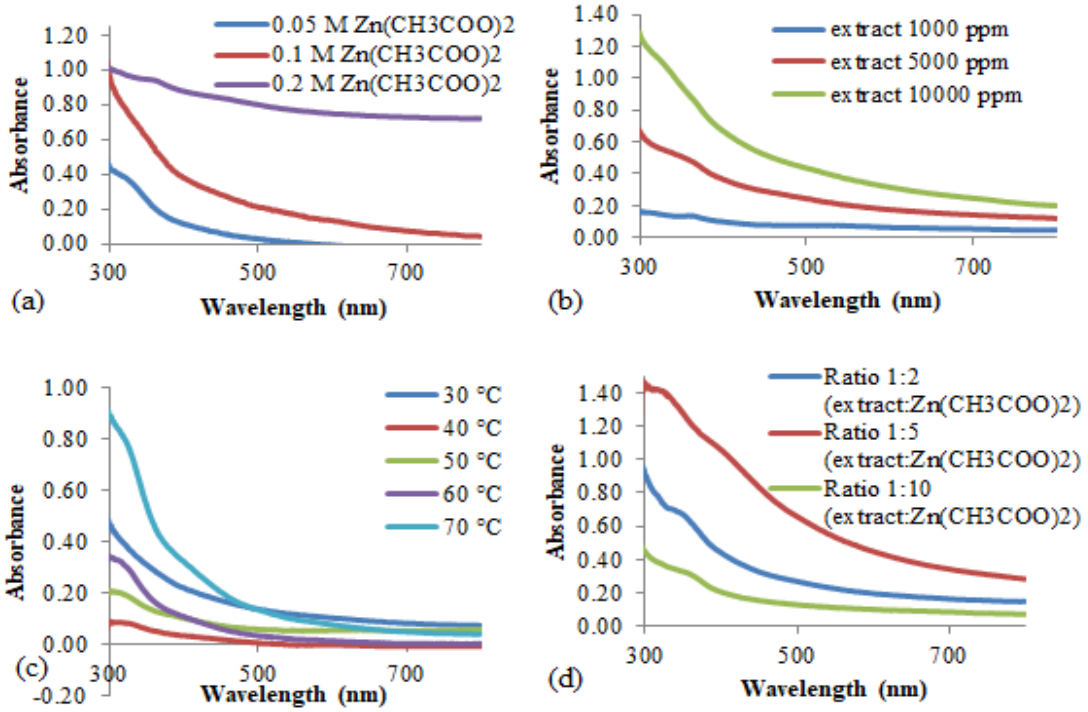

Figure 13. UV-Vis spectrum of ZnONP prepared at different condition:
(a) concentration of Zn $(CH_3COO)_2$ (b) concentration of aqueous *M. elengi* leaf extract (c) temperature (d) ratio of extract and $Zn(CH_3COO)$

First step to confirm the synthesise product to get ZnONP, can use UV-Vis spectrophotometer by determining the peak at around 370 nm that indicate the formation of ZnONP. It also can be knowing by the colour changing of solution from yellow brownish to white. The increasing concentration of zinc acetate and extract equals to the increasing absorbance. It's because higher concentration has higher silver ion and phenolic compound so there are many ZnONP can be formed. The increasing reaction time also make increasing absorbance because the particle reacts with other in longer time so will produce more particle of ZnONP than less reaction time. The increasing of temperature also makes the increasing of absorbance because with heating the solution so the reaction rate can be faster than in lower temperature. The AgNP synthesized product can be confirmed further by using UV-Visible spectrophotometer. The result showed at **Fig. 13** which showed the highest peak at 370 nm indicate the optimum condition to synthesis zinc oxide nanoparticle.

The FT-IR result of ZnONP at figure, which the band at 3425 cm^{-1} correspondence to O-H stretching H-bonded alcohol and phenol. The band at 1622 cm^{-1} correspondence to N-H bend primary amines. The band at 1385 cm^{-1} correspondence to C-O. The band at 1023 cm^{-1} correspondence to C-O-C stretching. The band at 541 cm^{-1} correspondence to ZnO bond at ZnONP. It also the comparison both of them at **Fig. 14**.

Research by Mirza et al. (2019) showed that to synthesize ZnONP using *Malus pumila* and *Juglen regia* aqueous leaf extract, for characterization using FTIR spectrum at 3464 cm^{-1} correspondence to O-H group of phenolic, 2928 cm^{-1} correspondence to amide, 1562 cm^{-1} correspondence to C=O of phenolic for *Juglen regia* extract. The band at 575 and 468 cm^{-1} correspondence to Zn-O in ZnONP. The highest peak around 500 cm^{-1} indicate the Zn-O bond from ZnONP. It can be know there are some shift of the peaks from higher to lower that indicate the ZnONP formation (Rad et al., 2019).

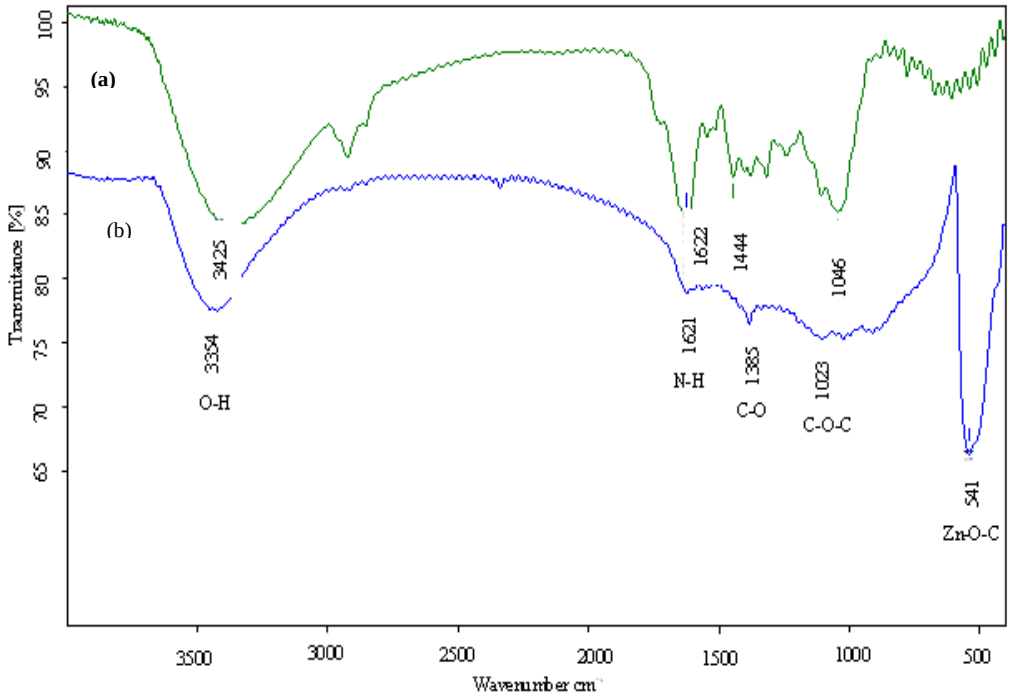

Figure 14. FTIR spectra of (a) *M. elengi* leaf (b) ZnONP

Next step, the crystallinity of ZnONP can be confirmed using powder XRD. Based on **Fig. 15.** showed the XRD pattern of ZnONP that prepared using *M.*

elengi leaf extract. There are some strong diffraction peaks at 2θ values of 31.7°, 34.4°, 36.2°, 47.5°, 56.6° and 62.8° which correspond to the (100), (002), (101), (102), (110) and (103) interplanar reflections of hexagonal crystal structure.

Research by Chandra et al. (2020) showed that to synthesize ZnONP using *Berberis aristata* aqueous leaf extract, for characterization using XRD showed the Bragg reflection peaks at 2θ values of 31.98°, 34.50°, 36.48°, 47.80°, 56.80°, 63.04°, 68.31° that was indexed to (101), (102), (110), (103), (200) and (112) planes structure of pure ZnOP (JCPDS, File No. 36-1451). So after comparing the high peaks with other similar research and from standard that can be knew that the ZnONP product from this research also has hexagonal crystal structure. The intense reflection of (101) peaks compare to other peaks indicate the nano crystal, like showed at **Fig. 15** (Sukri et al., 2019).

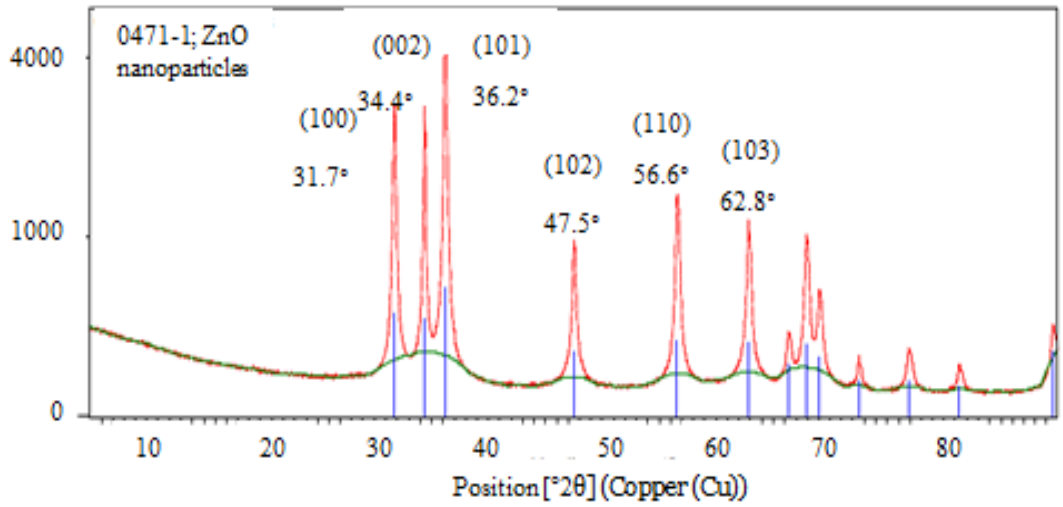

Figure 15. X-ray diffraction pattern of synthesized ZnONP

Last step to confirm the nanoparticle of sample by using transmission electron microscopy. Based on **Fig. 16** revealed that the particle size of ZnONP around 18.56 nm – 40.04 nm or the average of particle size around 28.44 nm. It can be confirmed that the ZnONP already at the range of nano size particle (1-100 nm).

Research by Mirza et al. (2019) showed that to synthesize ZnONP using *Malus pumila* and *Juglen regia* aqueous leaf extract, the characterization using TEM showed that the average of ZnONP particles size was 15 nm with rod shape. Besides that, can be known that phenolic and flavonoid compound from extract, was

coating the silver that have rod shapes, like showed at **Fig. 16** (Fahimmunisha et al., 2019). The particle size still in the range nano size (1-100 nm), so the ZnONP result from this research already formed in nano size.

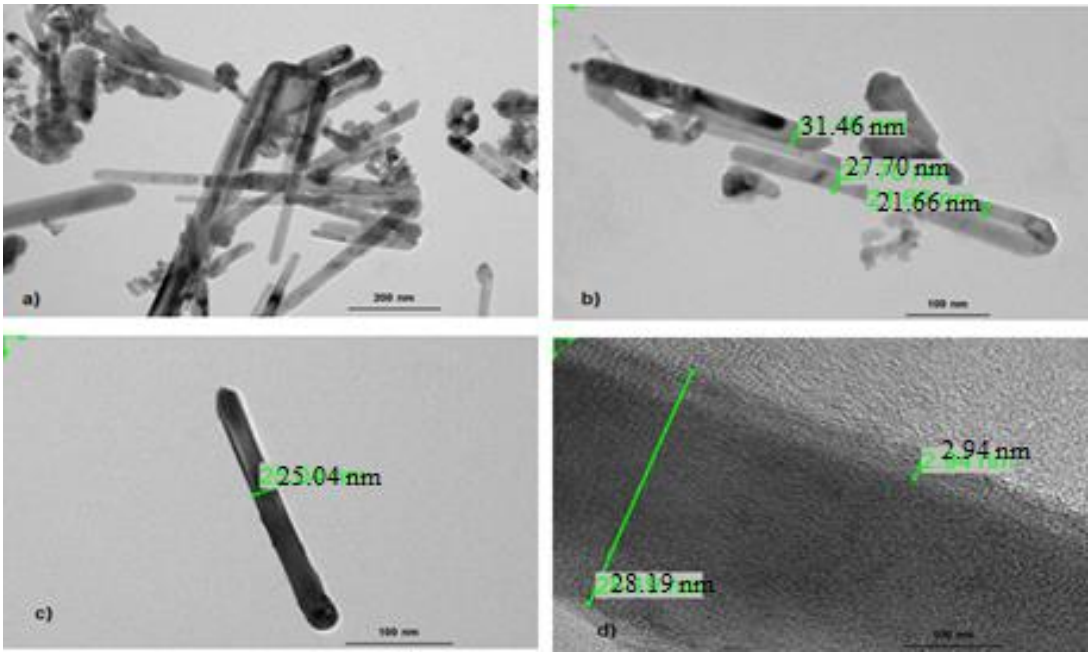

Figure 16. TEM images of ZnONP (a) particles at 200 nm (b) particles size at 100 nm (c) Rod shape (d) the coated NP

4.5 Antioxidant assay of extract and nanoparticles (AgNP and ZnONP)

The DPPH free radical is deep purple color of organic nitrogen radical. The color change from purple to yellow that indicate hydrazine formation when a DPPH solution being combined with an antioxidant. The reducing ability of antioxidants against DPPH can be determined by analyzing the decreasing of absorbance at 515– 528 nm. The results revealed the percentage of scavenging or IC_{50} of DPPH• for all the samples at a fixed antioxidant concentration.

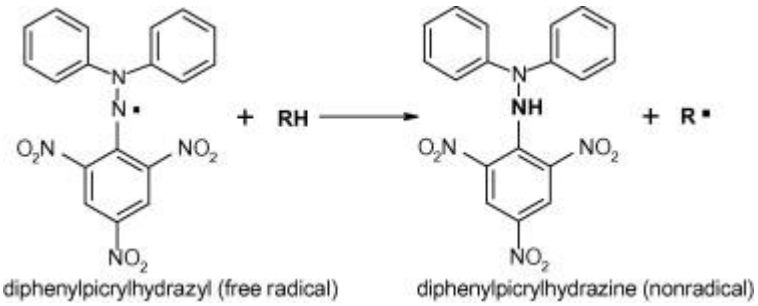

Figure 17. DPPH assay mechanism

Source: Paixao et al. (2007)

ABTS was being oxidized by manganese dioxide or potassium persulfate. The ABTS radical (ABTS•+) which have been absorbed at 743 nm (bluish green color) being formed by releasing an electron by the nitrogen atom of ABTS. In the presence of Trolox as hydrogen donating antioxidant, the nitrogen atom extinguished the hydrogen atom, yielding the decolorization of solution.

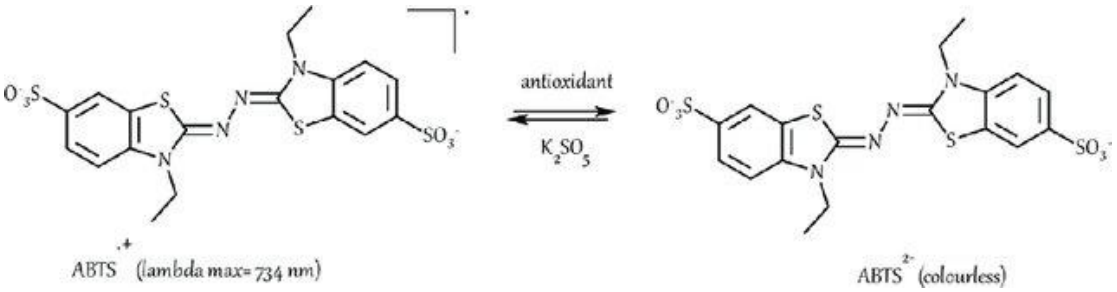

Figure 18. ABTS assay mechanism

Source: Sanchez et al. (2019)

The FRAP assay relies on the reduction of Fe3+–TPTZ (2,4,6-tri(2-pyridyl)-1,3,5-triazine) for producing Fe2+–TPTZ by the antioxidants. The bonding of Fe2+ with the ligand produce dark navy-blue color. The absorbance at 593 nm can be ued to examine the amount of iron reduced and can be correlated with the amount of antioxidant (Xiao et al., 2020).

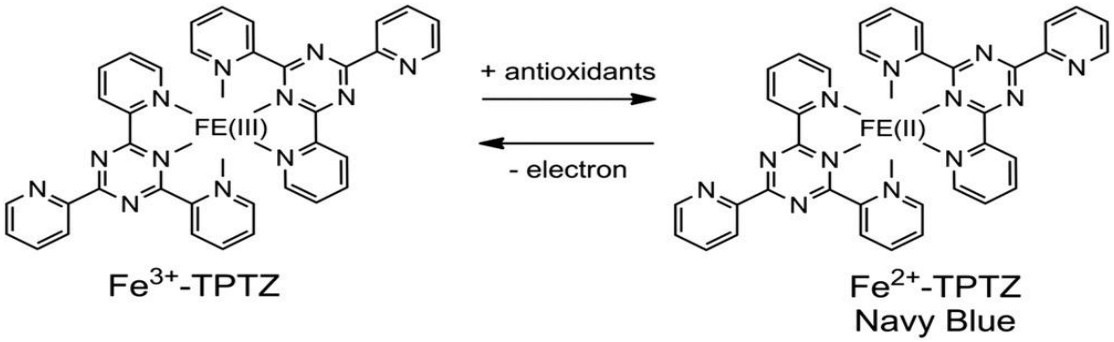

Figure 19. FRAP assay mechanism

Source: Xiao et al. (2020)

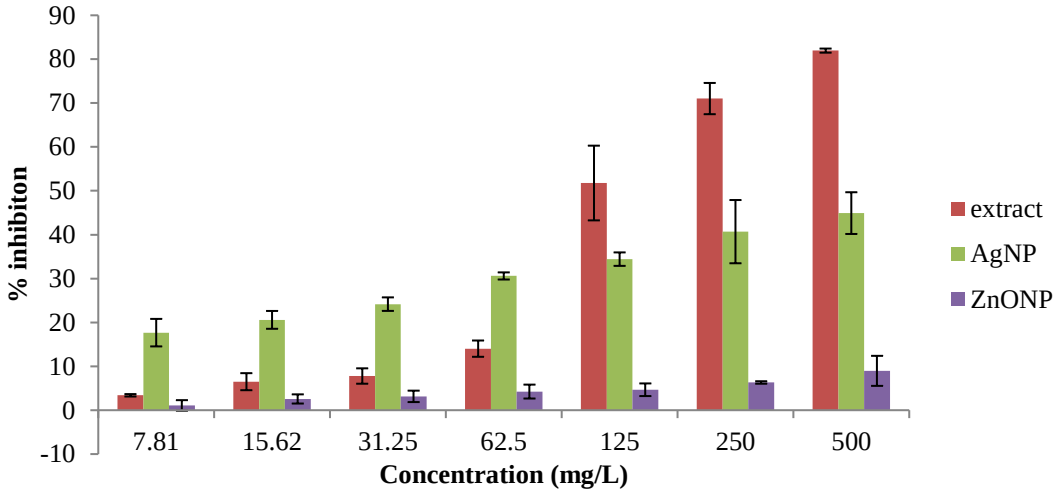

Figure 20. Percentage of inhibition by DPPH assay

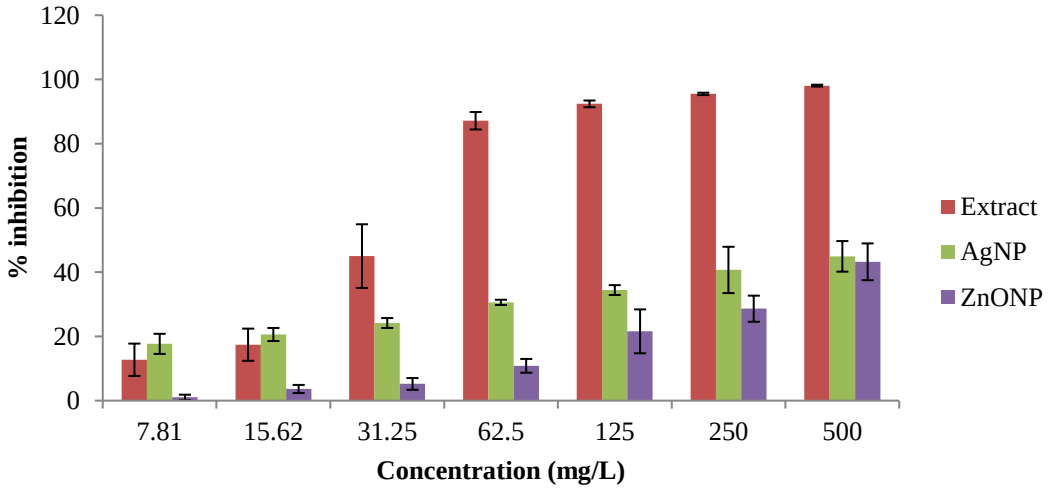

Figure 21. Percentage of inhibition by ABTS assay

The IC_{50} was calculated according to the following procedure: the respective regression line ($y = ax + b$) was drawn and inhibition ratios (y) were plotted against the sample concentrations (x) at all six points. The inhibition curve was slightly curved, so can be calculated the IC_{50} value applying the interpolation method by gathering the two points approximately at 50% inhibition with straight line as equation: a regression line ($Y = AX + B$) was drawn and two points enclosing a 50% inhibition ratio were selected. The regression equation of $Y = AX + B$, which X (sample concentration) being calculated by alternating the value of Y with 50 (Xiao et al., 2020)

Table 5. Antioxidant activity in *M. elengi* leaf

Sample	DPPH		ABTS		FRAP
	TEAC (mg/g)	**EC_{50} (mg/L)**	**TEAC (mg/g)**	**EC_{50} (mg/L)**	**(µM/mg)**
N1	436.37	131.43	328.93	32.84	4.29
N2	432.5	120.2	324.74	41.29	3.84
N3	431.69	168.28	327.52	39.1	3.97
Result	433.52 ± 2.50	139.97 ± 25.16	327.06 ± 0.58	37.34± 4.38	4.03± 0.23

The data about antioxidant activity in *M. elengi* leaf was shown at **Table 5**. Based on the table above can be knew that TEAC value from ABTS assay has higher value than DPPH assay, which 433.52 mg/g extract for DPPH assay and 332.25 mg/g extract for ABTS assay. The similar result as the EC_{50} value, for ABTS assay has higher value than DPPH assay, which 139.97 mg/L extract for ABTS assay and 37.34 mg/L extract for DPPH assay. For FRAP assay can be knew ferro reduction equivalent value is about 76.71 µM/mg extract.

Research by Natungnuy and Poeaim (2018) about antioxidant and cytotoxicity activities of methanolic extracts from *Mimusops elengi* flowers showed that EC_{50} value for ABTS assay has higher value than DPPH assay, which 236.13 mg/L extract for ABTS assay and 98.20 mg/L extract for DPPH assay. For FRAP assay can be knew ferro reduction equivalent value is about 63.11 µM/mM extract.

Thus, this study has lower EC_{50} value than previous study, which it indicate better antioxidant potential.

After that, the antioxidant potential of nanoparticles (AgNP and ZnONP) also have to determine. This is the data about antioxidant activity of AgNP at **Table6**. Based on the table above can be knew that TEAC value from ABTS assay has higher value than DPPH assay, which 233.88 mg/g extract for DPPH assay and 197.63 mg/g extract for ABTS assay. Same result as the EC_{50} value, for ABTS assay has higher value than DPPH assay, which 237.33 mg/L extract for ABTS assay and 215.45 mg/L extract for DPPH assay. For FRAP assay can be knew ferro reduction equivalent value is about 0.97 µM/mg extract.

Research by Wang et al. (2018) about characterization, antioxidant and antimicrobial activities of green synthesized silver nanoparticles from *Psidium guajava* L. leaf aqueous extract showed that EC_{50} value for ABTS assay has higher value than DPPH assay, which 55.10 mg/L extract for ABTS assay and 52.53 mg/L extract for DPPH assay. Thus, this study has higher EC_{50} value than previous study, which it indicate the antioxidant potential of AgNP product from this research was lower than previous study. It's because some of hydroxyl group of phenolic compounds already binding with silver ion so only less hydroxyl group that freely or still not bind, thus less hydroxyl group make the antioxidant activities also low.

Table 6. Antioxidant activity in AgNP

	DPPH		**ABTS**		
Sample	**TEAC (mg/g)**	**EC_{50} (mg/L)**	**TEAC (mg/g)**	**EC_{50} (mg/L)**	**FRAP (µM/mg)**
N1	229.94	204.55	198.83	211.96	1.06
N2	261.26	247.49	213.76	197.05	0.75
N3	210.43	259.95	180.33	236.54	1.11
Result	233.88± 25.65	237.33± 29.07	197.63± 16.76	215.45± 19.58	0.97 ± 0.19

This is the data about antioxidant activity of ZnONP at **Table 7** like below. Based on the table above can be knew that TEAC value from ABTS assay has higher value than DPPH assay, which 21.98 mg/g extract for DPPH assay and 24.74 mg/g extract for ABTS assay. Same result as the EC_{50} value, for ABTS assay has higher value than DPPH assay, which 5380.20 mg/L extract for ABTS assay and 2785.41 mg/L extract for DPPH assay. For FRAP assay can be knew ferro reduction equivalent value is about 0.09 µM/mg extract.

Research by Sonia et al. (2017) showed that to synthesize ZnONP using *Adhatoda vasica* aqueous leaf extract need showed that EC_{50} value for DPPH assay was 139.27 mg/L. Thus, this study has higher EC_{50} value than previous study, which it indicate the antioxidant potential of ZnONP product from this research was lower than previous study. It's because some of hydroxyl group of phenolic compounds already binding with silver ion so only less hydroxyl group that freely or still not bind, thus less hydroxyl group make the antioxidant activities also low.

Table 7. Antioxidant activity in ZnONP

	DPPH		**ABTS**		**FRAP**
Sample	**TEAC (mg/g)**	**EC_{50} (mg/L)**	**TEAC (mg/g)**	**EC_{50} (mg/L)**	**(µM/mg)**
N1	19.62	5856.2	24.86	2825.74	0.10
N2	21.66	5227.2	24.49	2958.97	0.09
N3	24.67	5057.2	24.94	2571.54	0.09
Result	21.98 ± 2.54	5380.20 ± 420.87	24.74 ± 0.24	2785.41 ± 196.84	0.09 ± 0.01

All of this can be occurred because the higher concentration so contains the higher phenolic compound in sample. Thus, there are many hydroxyl groups that react with free radical compound. Then, it gives the result that percent scavenging yet EC_{50} value of sample getting increase (Wang et al., 2018). Extract has the highest among of them.The AgNP has higher value than ZnONP. Generally, the phenolic compound that contain in extract and nanoparticles has potential as antioxidant.

4.6 Cytotoxicity of extract and nanoparticles (AgNP and ZnONP)

Tetrazolium salt solutions are colorless and change into a strong colored solution when forming the formazan product. In cell culture, the most commonly used tetrazolium salt is MTT (3-(4,5-dimethylthiazol-2-yl)-2,5-diphenyltetrazolium bromide) to measure proliferation and cytotoxicity for screening approaches in 96-well plates. Due to its lipophilic side groups and positive net charge MTT is able to pass the cell membrane. This results in a conversion of MTT to the water-insoluble formazan. The formation of formazan crystals destroys the cell and lead to cell death. Because the crystals are formed intracellularly, MTT-based assay protocols usually include a cell lysis step and a formazan-dissolving step before a spectroscopic measurement can be performed. It was rapid and simple, an assay for any real-time assays. (Prabst et al., 2017).

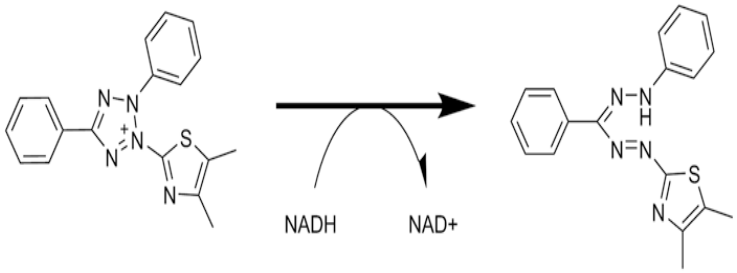

Figure 22. MTT assay mechanism

(Prabst et al., 2017)

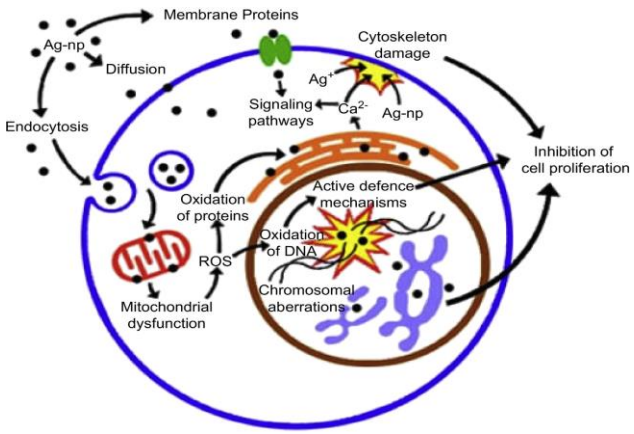

Figure 23. Mechanism of antioxidant using silver nanoparticles

Source: McShan et al. (2014)

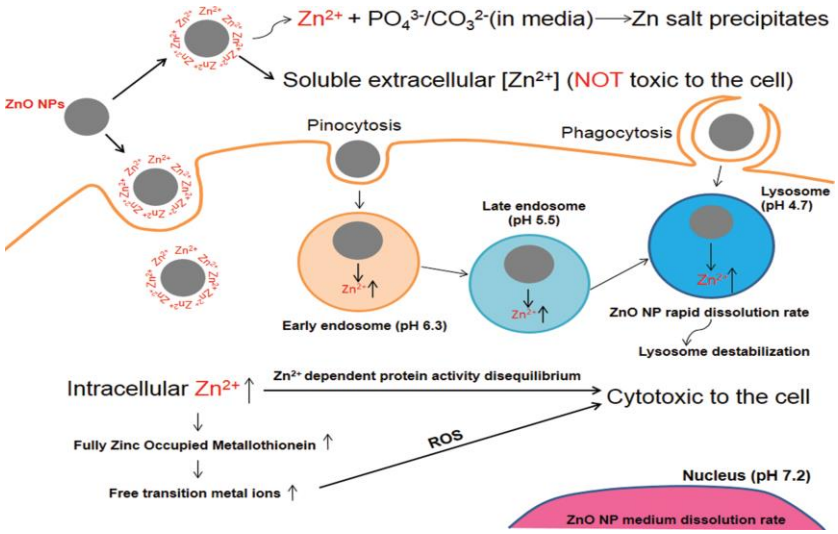

Figure 24. Mechanism of anticancer using zinc oxide nanoparticles

Source: Bisht and Rayamajhi (2016)

The last step about application of extract and nanoparticles beside antioxidant assay is cytotoxicity by determining the percentage of cell viability based on their concentration (Shanaz et al., 2019). At **Fig. 25** showed cytotoxicity of extract and nanoparticles against normal cell called Vero cell, using DMSO as control. At **Fig. 26** showed cytotoxicity of extract and nanoparticles against cancer cell called Caco-2 cell, using DMSO as control. Thus, can be known in normal cell, extract and nanoparticles make the increasing of percentage of viability cell. It's also has same result for cancer cell. Thus, extract and nanoparticles it's nontoxic and can make cell grow better.

Research by Gomaa (2017) showed that AgNP using Onion (*Allium cepa*) had antitumor activities against HCT-116 lines colon cancer and less effect to vero cell as normal cell, which had IC_{50} value about 2.2 µg/mL. Research by Shahnaz et al. (2019) showed that ZnONP also have same result, which ZnONP had antitumor activities against HCT-116 lines colon cancer and less effect to vero cell as normal cell, which had IC_{50} value about 20 µg/mL. The EC_{50} value from result higher than previous study. It indicate the anticancer potential from this research very low and almost no activity. Based on the result, extract has the highest cytotoxicity or anticancer potential among of nanoparticles (AgNP and ZnONP).

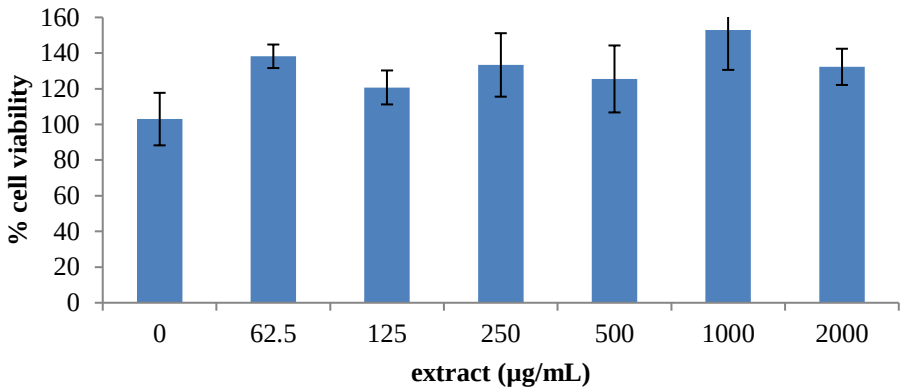

Figure 25. Percentage of cell viability against Vero cell of extract

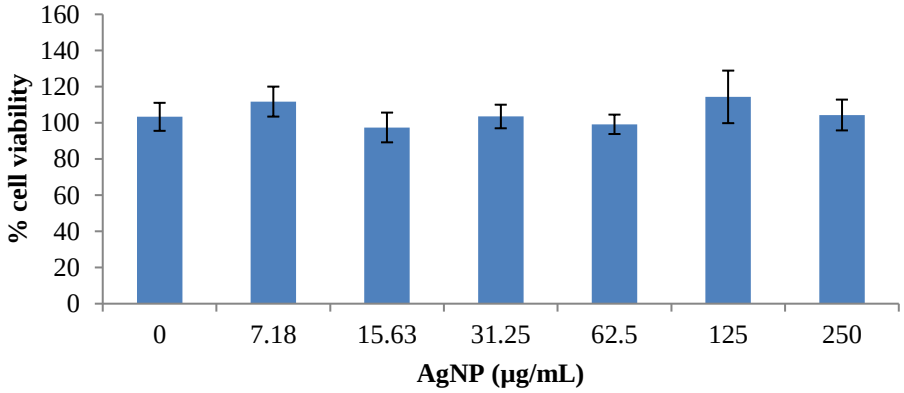

Figure 26. Percentage of cell viability against Vero cell of AgNP

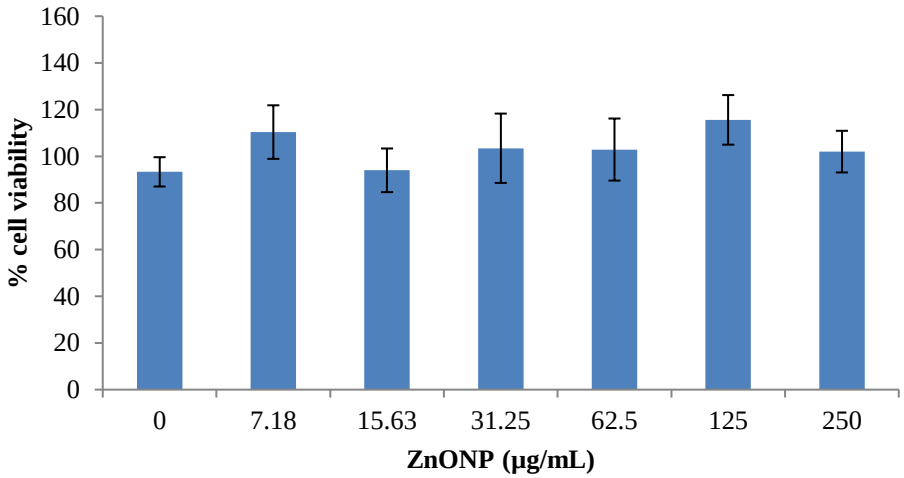

Figure 27. Percentage of cell viability against Vero cell of ZnONP

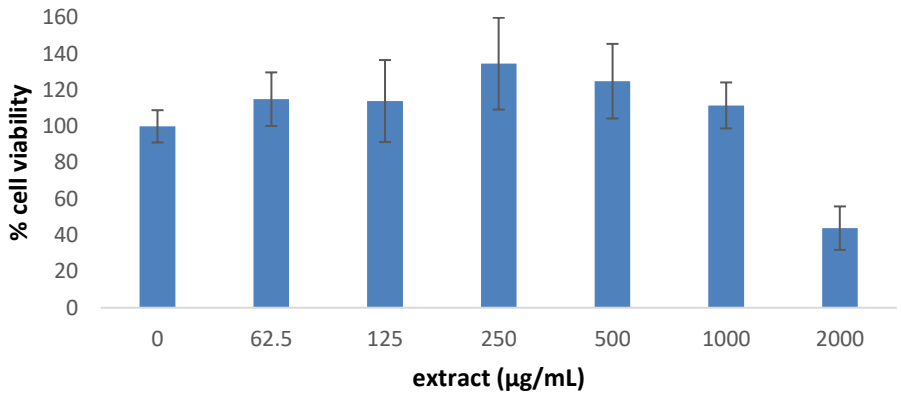

Figure 28. Percentage of cell viability against Caco-2 cell of extract

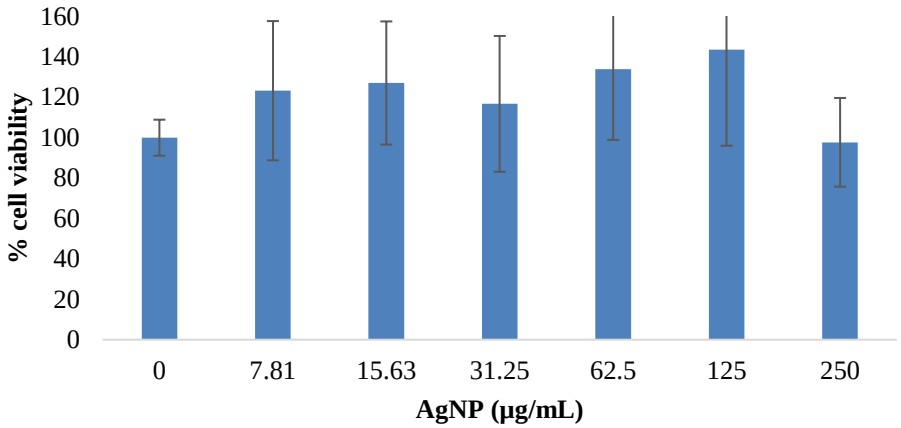

Figure 29. Percentage of cell viability against Caco-2 cell of AgNP

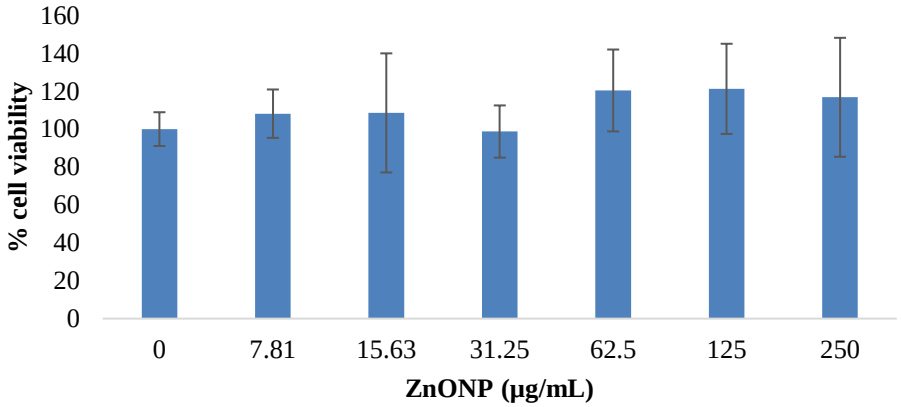

Figure 30. Percentage of cell viability against Caco-2 cell of ZnONP

The graph at **Fig. 25-30** showed that the increasing concentration of samples considered to the decreasing percentage of cell viability, because there were many particles that can acted against the cell. Thus, from this experiment revealed that the samples, extract and nanoparticles, have low potential as anticancer against colon cancer (Caco-2 cell) and no effect against normal cell (Vero cell).

CHAPTER 5
CONCLUSIONS AND RECOMMENDATIONS

CONCLUSION:

1. *M. elengi* leaves extract can be used to synthesized AgNP and ZnONP which AgNP has spherical shapes with the average of particle size 22.12 nm and ZnONP has rod shapes with the average particle size 28.44 nm.
2. *M. elengi* leaves extract has higher antioxidant and cytotoxicity activity than the nanoparticles (AgNP and ZnONP).
3. Both of nanoparticles (AgNP and ZnONP) are nontoxic against Vero (normal cell) and Caco-2 (colon cancer cell), but extract at 2000 ppm is toxic against Caco-2 cell and nontoxic against Vero cell.

SUGGESTION:

1. M. *elengi* leaves extract at higher concentration, 2000 ppm, can be used as anti-cancer against colon cancer, Caco-2.
2. Both of nanoparticles (AgNP and ZnONP) can be used in other application such as for cosmetic product, because nontoxic against normal and cancer cell.

REFERENCES

Ahmad, N. and Sharma, S. 2012. Green Synthesis of Silver Nanoparticles Using Extracts of *Ananas comosus.* Green and Sustainable Chemistry.2, 141-147.

Ahmed, S., Annu, Chaudhry, S.A. and Ikram, S. 2017. A review on biogenic synthesis of ZnO nanoparticles using plant extracts and microbes: A prospect towards green chemistry. Journal of Photochemistry and Photobiology, B: Biology. 166 (2017) 272–284.

Annavaram, V., Posa V.R., Uppara, V.G., Jorepalli, S. and Somala, A.R. 2015. Facile green synthesis of silver nanoparticles using *Limonia Acidissima* leaf extract and its antibacterial activity. Biological of Nanoscience. 5, 97–103.

Awwad, A.*M.*and Salem, N.*M.*2012. A green and facile approach for synthesis of magnetitenanoparticles. Nanoscience and Nanotechnology. 2, 208–213.

Babu, E. P., Subastri, A., Suyavaran, A., Rao. P.L., Kumar, M.S., Jeevaratnam, K., and Thirunavukkarashu, C. 2015. Extracellularly synthesized ZnO nanoparticles interact with DNA and augment gamma radiation induced DNA damage through reactive oxygen species. *The Royal Society of Chemistry Advance*. RSC. London, UK, pp. 62070.

Bakar, M.F., Mohamed, *M.*and Rahmat, A. 2009. Phytochemicals and antioxidant activities of edible herbs. Journal of Food Chemistry. 113, 479-483.

Baliga, M.S., Pai, R.J., Bhat, H.P., Palatty P.L. and Boloor, R. 2011. Chemical and medicinal properties of Bakul (*Mimusops elengi* Linn): a review. Food Research International. 44, 1823-1829.

Bartosz, G. 2013. Food oxidants and antioxidants chemical, biological and functional properties. CRC Press, Taylor and Francis Group. Florida, USA, pp. 568.

Benzie, I.F. and Strain, J.J. 1996. The ferric reducing ability of plasma (FRAP) as a measure of "antioxidant power": the FRAP assay. Analitical Biochemistry. 239, 70-76.

Bisht, G. and Rayamajhi, S. 2016. ZnO Nanoparticles: a promising anticancer agent. Nanobiomedicine. 1-11.

Burt, R.W. 2000. Colon cancer screening. Gastroenterology Special Reports and Reviews. 119, 837–853.

Chandra, H., Kumari, P., Bontempi, E. and Yadav, S. 2020. Medicinal plants: Treasure trove for green synthesis of metallic nanoparticles and their biomedical applications. Biocatalysis and Agricultural Biotechnology. 24 (2020) 101518.

Das, D., Nath B.C., Phukon, P., Kalita, A. and Dolui, S.K. 2013. Synthesis of ZnO nanoparticles and evaluation of antioxidant and cytotoxic activity. Colloids and Surfaces B: Biointerfaces 111, 556– 560.

El-Nour, K.M.M.A., Eftaiha, A., Al-Warthan, A. and Ammar, R.AA. 2010. Synthesis and applications of silver nanoparticles. Arabian Journal of Chemistry. 3, 135–140.

Fafal, T., Taştan, P., Tüzüna, P.S., Ozyazici *M.*and Kivcak. B. 2017. Synthesis, characterization and studies on antioxidant activity of silver nanoparticles using Asphodelus aestivus Brot. aerial part extract. South African Journal of Botany. 112, 346–353.

Fahimmunisha, B.A., Ishwarya, R., Al-Salhi, M.S., Devanesan, S., Govindarajan, *M.*and Vaseeharan, B. 2019. Green fabrication, characterization and antibacterial potential of zinc oxide nanoparticles using *Aloe socotrina* leaf extract: A novel drug delivery approach. Journal of Drug Delivery Science and Technology 55 (2020) 101465.

Gadamsetty, G., Maru, S. and Sarada, N.C. 2013. Antioxidant and anti-inflammatory activities of the methanolic leaf extract of traditionally used medicinal plant *Mimusops elengi* L. Journal of Pharmaceutical Sciences and Research. 5 (6), 125–130.

Gami, B., Pathak, S. and Parabia, *M.*2012. Ethnobotanical, phytochemical and pharmacological review of *Mimusops elengi* Linn. Asian Pacific Journal of Tropical Biomedicine. 2(9), 743-748.

Gopalkrishnan, B. and Shimpi, S.N. 2012. *Mimusops elengi*: a review on ethnobotany, phytochemical and pharmacological profile. International Journal of Pharmacognosy Phytochemistry Research. 3, 13–17.

Gomaa, E.Z. 2017. Antimicrobial, antioxidant, and antitumor activities of silver nanoparticles synthezied by *Allium cepa* extract: A green approach. Journal of Genetic Engineering and Biotechnology. 15 (2017) 49-57.

Hayouni E.A, Abedrabba M., Bouix *M.*and Hamdi *M.*2007. The effects of solvents and extraction method on the phenolic contents and biological activities in vitro of *Tunisian Quercus coccifera* L. and *Juniperus phoenicea* L. fruit extracts. Food Chemistry 105 (2007) 1126–1134

Havlicek, V. and Spizek, Z. 2014. Natural Product Analysis: Instrumentation, Method, and Application. John Wiley and Sons. Canada, America, pp. 1-9.

Hu, D., Si W, B., Qin, W., Jiao, J., Li, X.L., Gu, X.P. and Hao, Y.F. 2019. *Cucurbita pepo* leaf extract induced synthesis of zinc oxide nanoparticles, characterization for treatment of femoral fracture. Journal of Photochemistry and Photobiology, B: Biology. 195 (2019) 12-16.

Iravani, S. 2011. Green synthesis of metal nanoparticles using plants. Green Chemistry. 13, 2638–2650.

Karmakar, U.K., Sultana, R. and Biswas, N.N., 2011. Antioxidant, analgesic and cytotoxic activities of *Mimusops elengi* Linn. *leaf*. International Journal of Pharmaceutical Sciences and Research. 2 (11), 2791-2797.

Khalil, M.M.H, Ismail, E.H., El-Baghdady, K.Z. and Mohamed D., 2013. Green synthesis of silver nanoparticles using *olive* leaf extract and its antibacterial activity. Arabian Journal of Chemistry. 7(6), 1131-1139

Kumar, H.A.K., Mandal, B.K., Kumar, K.M., Maddinedi, S.B., Kumar, T.S., Madhiyazhagan, P. and Ghosh, A.R. 2014. Antimicrobial and antioxidant activities of *Mimusops elengi* seed extract mediated isotropic silver nanoparticles. Spectrochimica Acta Part A: Biomolecular Spectroscopy. 130, 13–18.

Lane, N., National Nanotechnology Initiative: The initiative and its implementation plan. 2000. National Science and Technology Council, Committee on Technology, Subcommittee on Nanoscale Science, Engineering and Technology, Washington DC, July 11, 2000, 19-20.

Larkin, P.J. 2011. IR and Raman Spectroscopy: Principle and Spectral Interpretation. Elsevier. Amsterdam, Netherland, pp. 1-7.

Lichota, A. and Gwozdzinski, K. 2018. Anticancer activity of natural compounds from plant and marine environment. International Journal Molecular Science. 19, 3533.

Liu, J.L. and Bashir, S. 2015. Advance Nanomaterials and Their Applications in Renewable Energy. Elsevier. Amsterdam, Netherland, pp. 121-166.

McShan, D., Ray, P.C. and Yu, H. 2014. Molecular toxicity mechanism of nanosilver. Journal of Food and Drug Analysis. 22, 116-127.

Natungnuy, K. and Poeaim, S. 2018. Antioxidant and cytotoxicity activities of methanolic extracts from *Mimusops elengi* flowers. International Journal of Agricultural technology, 14: 731-740.

Pasupuleti, V.R., Prasad, T., Shiekh, R.A., 2013. Biogenic silver nanoparticles using *Rhinacanthus nasutus* leaf extract, synthesis, spectral analysis, and antimicrobial studies. International Journal of Nanomedicine. 8, 3355–3364.

Paixao, N., Perestrelo, R., Marques, J.C. and camara, J.S. 2007. Relationship between antioxidant capacity and total phenolic content of red, rose´ and white wines. Food Chemistry. 105 (2007) 207.

Poole, C.P. and Owens, F.J. Introduction to Nanotechnology. 2003. A John wiley Inter-science Publication. New Jersey, USA, pp. 1-2.

Prabst, K., Engelhardt, H., Ringgeler, S., Hubner, H., 2017. Cell Viability Assays: Methods and Protocols, Methods in Molecular Biology. Berlin, Germany, pp. 3.

Prakash, P., Gnanaprakasam, P., Emmanuel, R., Arokiyaraj, S. and Saravanan, *M.*2013. Green synthesis of silver nanoparticles from leaf extract of *Mimusops elengi* Linn. for enhanced antibacterial activity against multi drug resistant clinical isolates. Colloids and Surfaces B: Biointerfaces. 108, 255– 259.

Rad, S.S., Sani, A.*M.*and Mohseni, S. 2019. Biosynthesis, characterization and antimicrobial activities of zinc oxide nanoparticles from leaf extract of *Mentha pulegium* (L.). Microbial Pathogenesis 131 (2019) 239–245.

Radojkovic, M., Zekovic, Z., Maskovic, P., Mandic, S.V.A, Misan A and Durovic, S. 2016. Biological activities and chemical composition of *Morus leaf* extracts obtained by maceration and supercritical fluid extraction. J. of Supercritical Fluids 117, 50-58.

Rao, K.S., Munjuluri, P.*M.*and Keshar, N.K. 2011. Invitro antioxidant activity and total phenolic content of *Mimusops elengi* bark. Indian Journal of Pharmaceutical Education Research. 45, 4.

Re, R., Pellegrini, N., Proteggente, A., Pannala, A., Yang, *M.*and Evans, C.R. 1999. Antioxidant activity applying an improved ABTS radical cation decolorization assay. Free Radical Biological Medicine. 26, 1231-1237.

Roby, M.H.H, Srahan, M.A., Selim, K.A.H and Khalel, K.I. 2013. Evaluation of antioxidant activity, total phenol and phenolic compounds in thyme (*Tyhmus vulgaris* L.), sage (*Salvia Officinalis* L.), and marjoram (*Origanum majorana* L.) extracts. Industrial Crops and Products. 43 (2013) 827-831.

Rosa G.S.D, Vanga S.K., Gariepy Y. and Raghavan V. 2019. Comparison of microwave, ultrasonic and conventional techniques for extraction of bioactive compounds from olive *leaf* (*Olea europaea* L.). Innovative Food Science and Emerging Technologies 58 (2019) 102234.

Sahu, S.C. 2016. Altered global gene expression profiles in human gastro intestinal epithelial Caco-2 cells exposed to nanosilver. Toxicology Reports. 3, 262–268.

Sanchez, N.F.S., Coronado, R.S., Canongo, C.V and Carlos B.H. 2019. Antioxidant Compounds and Their Antioxidant Mechanism. Antioxidants. 3 (2019), 19.

Sharmila, G., Thirumarimurugan, *M.*and Muthukumaran, C. 2019. Green synthesis of ZnO nanoparticles using *Tecomacas tanifolia* leaf extract: Characterization and evaluation of its antioxidant, bactericidal and anticancer activities. Microchemical Journal. 145, 578–587.

Sangaonkar, G. and Pawar, K.D. 2018. *Garcinia indica* mediated biogenic synthesis of silver nanoparticles with antibacterial and antioxidant activities. Colloids and Surfaces B: Biointerfaces 164 (2018) 210–217.

Shahnaz, M., Danish, M., Ismail, M.H.B., Ansari, M.T. and Ibrahim, M.N.*M.*2019. Anticancer and apoptotic activity of biologically synthesized zinc oxide nanoparticles against human colon cancer HCT-116 cell line- in vitro study. Sustainable Chemistry and Pharmacy 14 (2019) 100179.

Singh, A., Gautam, P.K., Verma, A., Singh, V., Shivapriya, P.M., Shivalkar, S., Sahoo, K. and Samanta, S.K. 2020. Green synthesis of metallic nanoparticles as

effective alternatives to treat antibiotics resistant bacterial infections: A review. Biotechnology Reports. 25 (2020) 100427.

Singleton, V.L., Orthofer, R. and Raventós, R.M.L. 1999. Analysis of total phenols and other oxidation substrates and antioxidants by means of Folin-Ciocalteu reagent. Methods Enzymol. 299, 152-178.

Sirkar, K.K. 2012. *Current opinion in chemical engineering*. Elsevier. Amsterdam, Netherland, pp. 123-128.

Sisodiya, P.S. 2013. Plant derived anticancer agents: a review. International Journal Research of Develeopment Pharmaceutical Science. 2, 293-308.

Sonane, M., Moin, N. and Satish, A. 2017. The role of antioxidants in attenuation of *Caenorhabditis elegans* lethality on exposure to TiO_2 and ZnO nanoparticles. Chemosphere. 187, 240-247.

Sonia, S., Kumari, L.J.H, Ruckmani, K. and Sivakumar, *M*.2017. Antimicrobial and antioxidant potentials of biosynthesized colloidal zinc oxide nanoparticles for a fortified cold cream formulation: A potent nanocosmeceutical application. Material Science and Engineering C. 79, 581-589.

Sruthi, S., Ashtami, J. and Mohanan, P.V. 2018. Biomedical application and hidden toxicity of zinc oxide nanoparticles. Material Today. 10, 175-186.

Sukri, S.N.M., Shameli, K., Wong, M.M.T, Teow, S.Y., Chew, J. and Ismail, N.A. 2019. Cytotoxicity and antibacterial activities of plant-mediated synthesized zinc oxide (ZnO) nanoparticles using *Punica granatum* (pomegranate) fruit peels extract. Journal of Molecular Structure 1189 (2019) 57-65.

Vijayakumar, S., Mahadevana, S., Arulmozhia, P., Sriramb, S. and Praseethac, P.K. 2018. Green synthesis of zinc oxide nanoparticles using Atalantia monophylla leaf

extracts: Characterization and antimicrobial analysis. Materials Science in Semiconductor Processing. 82, 39–45

Wang, L., Wu, Y., Xie, J., Wu, S. and Wu, Z. 2018. Characterization, antioxidant and antimicrobial activities of green synthesized silver nanoparticles from *Psidium guajava* L. leaf aqueous extracts. Materials Science & Engineering C 86 (2018) 1–8.

Xiao, F., Xu, T., Lu, B., and Liu, R. 2020. Guidelines for antioxidant assays for food components. Food Frontiers. 1,63.

Xu, J., Mao. W. 2016. Overview of research and development for anticancer drugs. Journal of Cancer Therapy. 7, 762-772.

Zare, M., Namratha, K., Byrappa K., Surendra, D.M., Yallappa, S. and Hungund, B. 2018. Surfactant assisted solvothermal synthesis of ZnO nanoparticles and study of their antimicrobial and antioxidant properties. Journal of Materials Science and Technology. 34, 1035–1043.

Zhang, X.F., Liu, Z.G., Shen, W. and Gurunathan, S. 2016. Silver Nanoparticles: Synthesis, Characterization, Properties, Applications, and Therapeutic Approaches. International Journal of Molecular Science. 17 (2016) 1534.

APPENDICES

Appendix 1

Sample preparation

(a)

(b)

(c)

(d)

(e)

Figure 31. *M. elengi* (a) cut and dried leaf (b) powder of leaf (c) macerated (d) filtrate (e) crude extract

Appendix 2

Determination of phytochemical

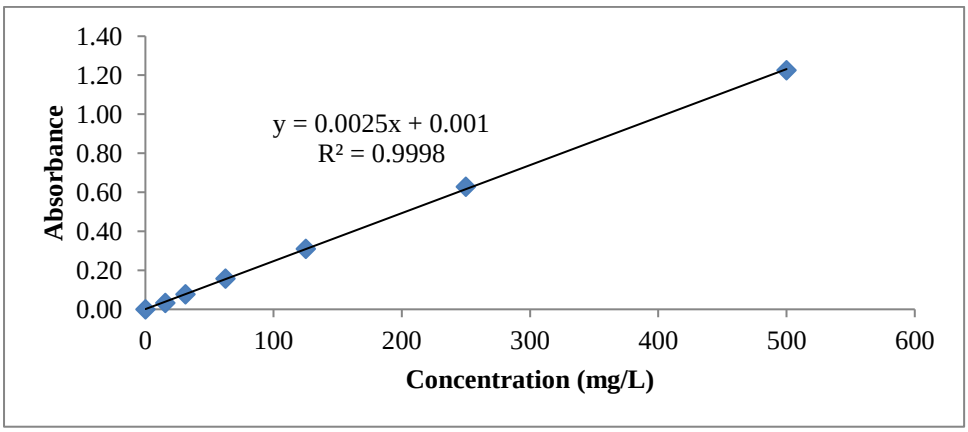

Figure 32. Gallic acid standard curve for total phenolic determination

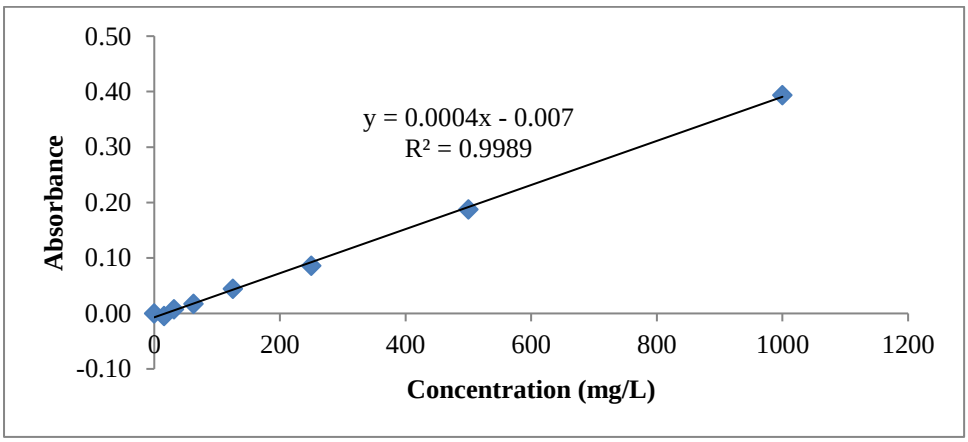

Figure 33. Catechin standard curve for total flavonoid content determination

Appendix 3

Determination of phytochemical (cont.)

(a) (b)

Figure 34. Phytochemical determination (a) TPC with gallic acid standard (15.625-1000 mg/L) (b) TFC with catechin standard (15.625-1000 mg/L)

Appendix 4

Determination of phytochemical (cont.)

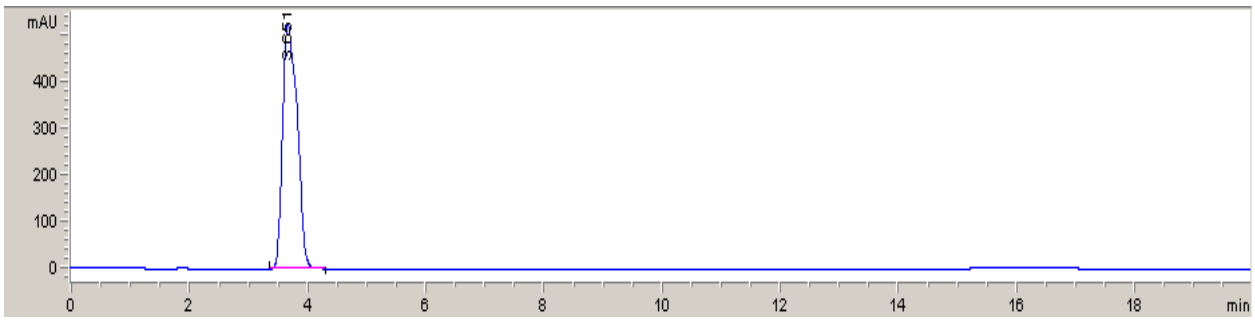

(a)

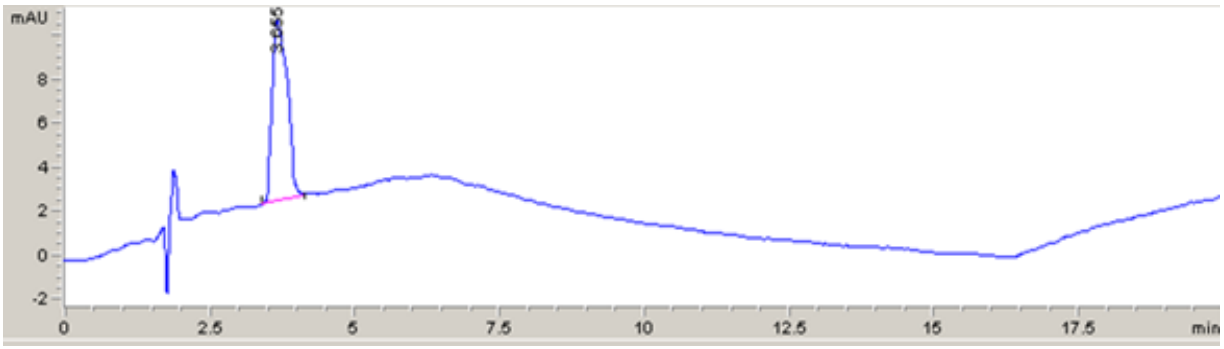

(b)

Figure 35. Chromatogram of Galic acid (a) standard (b) *M. elengi* leaf extract

Appendix 5

Figure 36. FT-IR Spectra of *M. elengi* Linn. aqueous leaf extract

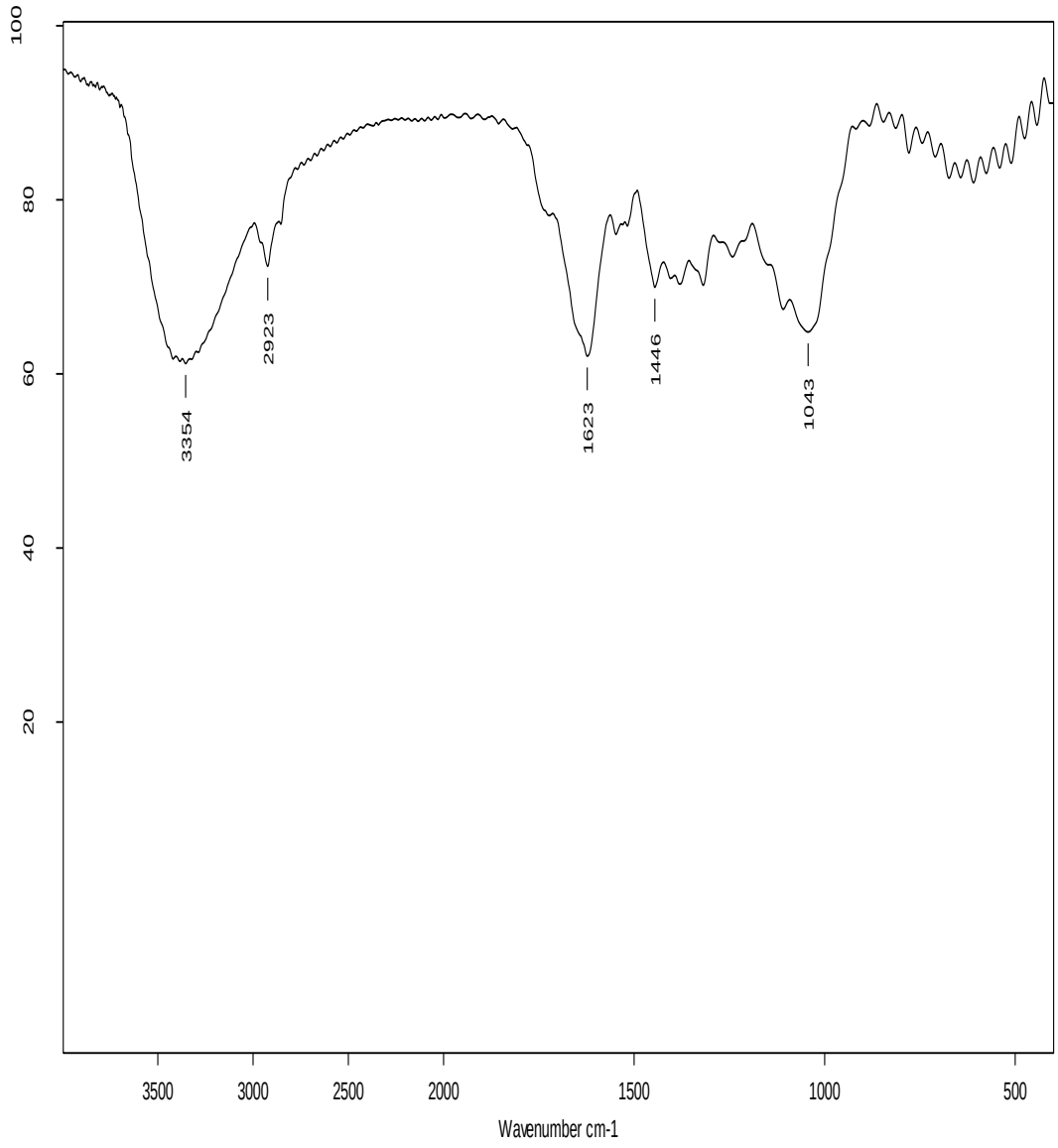

D:\IR spectrum\2562\Selly\Mimusops elengi (ME) leaves powder.0	Mimusops elengi (ME) leaves powder	Instrument type and / or acces	10/21/2019

Appendix 6

Figure 37. FT-IR Spectra of AgNP

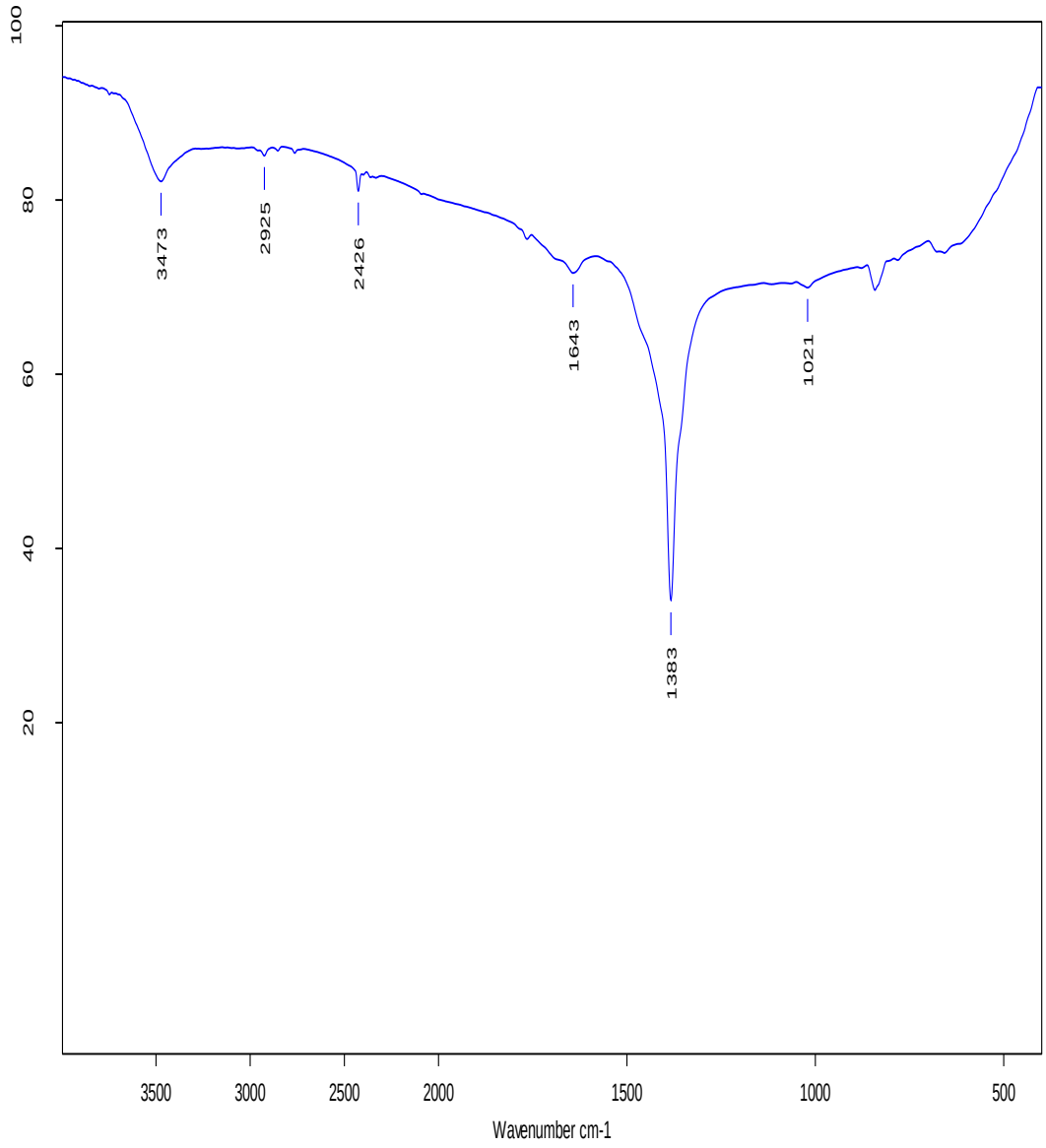

D:\IR spectrum\2562\Selly\silver nano (AgNp).5	silver nano (AgNp)	Instrument type and / or accessory	10/21/2019

Appendix 7

Figure 38. FT-IR Spectra of ZnONP

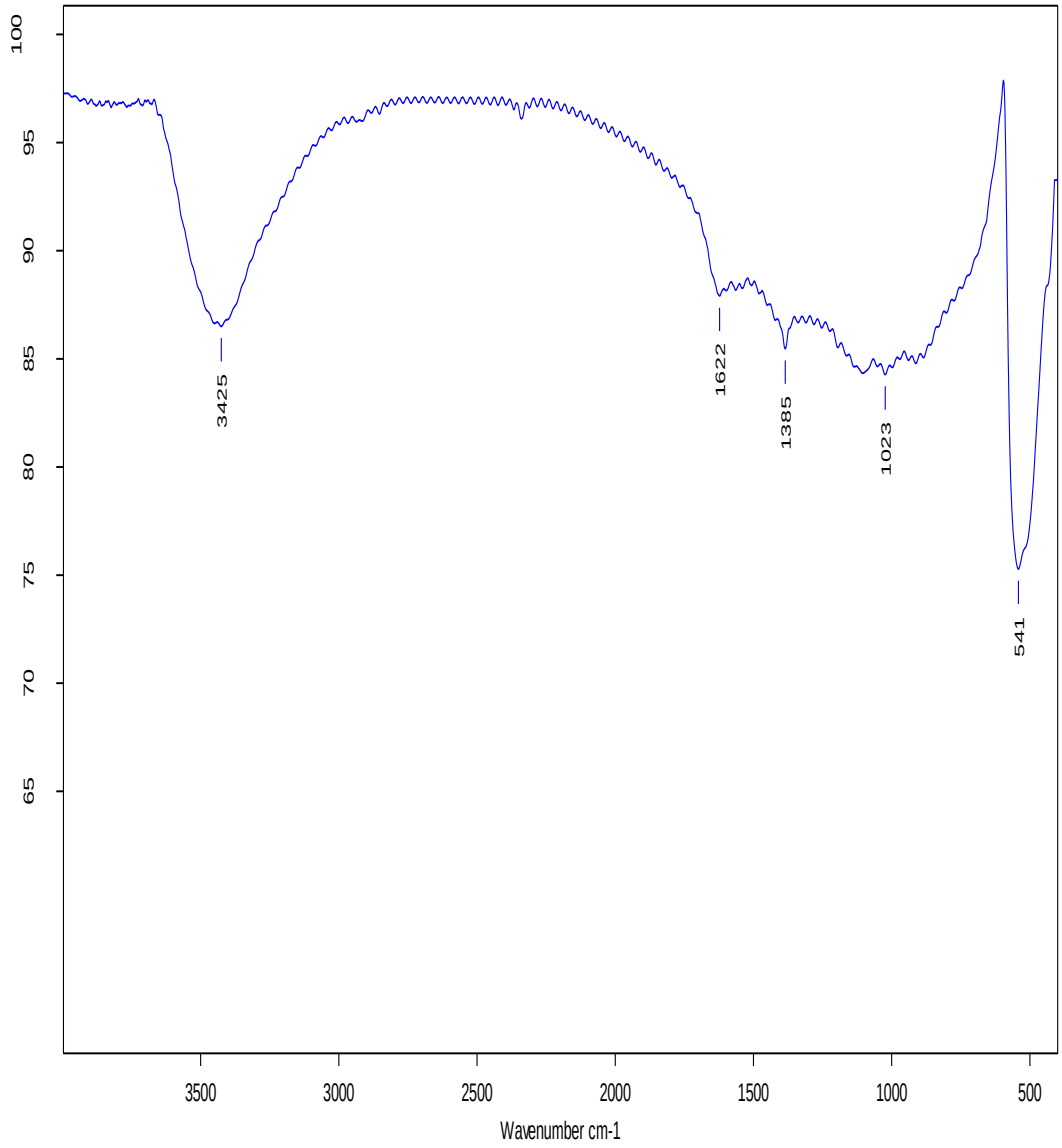

D:\IR spectrum\2563\Selly\zinc oxide nanoparticle.0	zinc oxide nanoparticle	Instrument type and / or accessory	2/7/2020

Appendix 8

Table 8. XRD data of AgNP

Date: 12/23/2019 Time: 11:27:54 AM File: HighScore Plus - 5058-1 User: DKSH1326103

Name and formula

Reference code:	01-087-0597
Mineral name:	Silver-3C, syn
Compound name:	Silver
Empirical formula:	Ag
Chemical formula:	Ag
Mineral classification:	Gold (Supergroup), 1C-disordered (Group)

Crystallographic parameters

Crystal system:	Cubic
Space group:	Fm-3m
Space group number:	225
a (Å):	4.0862
b (Å):	4.0862
c (Å):	4.0862
Alpha (°):	90.0000
Beta (°):	90.0000
Gamma (°):	90.0000
Volume of cell (10^6 pm^3):	68.23
Z:	4.00
RIR:	17.20

Status, subfiles and quality

Status:	Alternate Pattern
Subfiles:	Alloy, metal or intermetallic, Common Phase, Forensic, ICSD Pattern, Inorganic, Mineral, Mineral - Mineral, Mineral - Synthetic
Quality:	Indexed (I)

Comments

ANX:	N
ICSD collection code:	64706
Creation Date:	9/1/2000
Modification Date:	9/1/2011
Cross-References:	ICSD:64706
ANX:	N
Analysis:	Ag1
Formula from original source:	Ag
ICSD Collection Code:	64706
Melting Point:	M.p. 1235.1 K
Calculated Pattern Original Remarks:	Cell from 2nd reference at 298 K: 4.08621(12). Minor Warning: No e.s.d reported/abstracted on the cell dimension. No R factors reported/abstracted. Wyckoff Sequence: a(FM3-M). Unit Cell Data Source: Single Crystal.

References

Primary reference:	Calculated from ICSD using POWD-12++, (1997)
Structure:	Swanson, H.E., Tatge, E., Natl. Bur. Stand. (U. S.), Circ. 539, **539**, 1, (1953)

Peak list

No.	h	k	l	d [Å]	2θ [°]	I [%]
1	1	1	1	2.35917	38.114	100.0
2	2	0	0	2.04310	44.299	46.3
3	2	2	0	1.44469	64.443	23.2
4	3	1	1	1.23204	77.397	23.0
5	2	2	2	1.17958	81.541	6.4
6	4	0	0	1.02155	97.885	2.7
7	3	3	1	0.93744	110.512	8.2
8	4	2	0	0.91370	114.928	7.8
9	4	2	2	0.83409	134.892	6.7

Appendix 9

Table 9. XRD data of ZnONP

Date: 2/3/2020 Time: 2:16:08 PM File: HighScore Plus - 0471-1 User: DKSH1326103

Name and formula

Reference code:	01-078-2585
Mineral name:	Zincite, syn
Compound name:	Zinc Oxide
Empirical formula:	OZn
Chemical formula:	ZnO
Mineral classification:	Wurtzite (Supergroup), 2H (Group)

Crystallographic parameters

Crystal system:	Hexagonal
Space group:	P63mc
Space group number:	186
a (Å):	3.2522
b (Å):	3.2522
c (Å):	5.2095
Alpha (°):	90.0000
Beta (°):	90.0000
Gamma (°):	120.0000
Volume of cell (10^6 pm^3):	47.72
Z:	2.00
RIR:	5.21

Status, subfiles and quality

Status:	Alternate Pattern
Subfiles:	Alloy, metal or intermetallic, Ceramic, Ceramic - Semiconductor, Common Phase, Excipient, Forensic, ICSD Pattern, Inorganic, Mineral, Mineral - Mineral, Mineral - Synthetic, Pharmaceutical, Thermoelectric Material
Quality:	Star (S)

Comments

ANX:	AX
ICSD collection code:	164209
Creation Date:	9/1/2011
Cross-References:	ICSD:164209
ANX:	AX
Analysis:	O1 Zn1
Formula from original source:	Zn O
ICSD Collection Code:	164209
Calculated Pattern Original Remarks:	The sample with composition Zn0.976 Al0.024 O segregates into two phases: Zn O and Zn Al2 O4 (ICSD 164210). Sample Source or Locality: synthetic. Temperature of Data Collection: 293 K. Wyckoff Sequence: b2 (P63MC). Unit Cell Data Source: Powder Diffraction.

References

Primary reference:	Calculated from ICSD using POWD-12++
Structure:	Nie Dengpan, Xue Tao, Zhang Yu, Li Xiangjun, Sci. China,Ser. B:Chem., **51**, 823, (2008)

Peak list

No.	h	k	l	d [Å]	2θ [°]	I [%]
1	1	0	0	2.81652	31.744	55.8
2	0	0	2	2.60477	34.402	41.6
3	1	0	1	2.47760	36.228	100.0
4	1	0	2	1.91234	47.507	21.3
5	1	1	0	1.62612	56.550	30.1
6	1	0	3	1.47815	62.815	25.7
7	2	0	0	1.40826	66.321	3.9
8	1	1	2	1.37939	67.895	20.7
9	2	0	1	1.35947	69.029	10.2
10	0	0	4	1.30239	72.520	1.6
11	2	0	2	1.23880	76.897	3.1
12	1	0	4	1.18212	81.328	1.5

Appendix 10

Antioxidant Assay

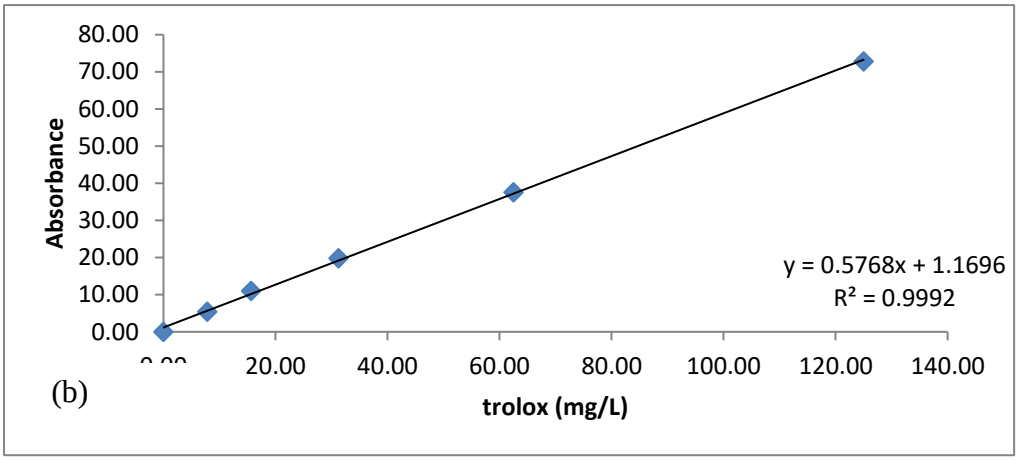

Figure 39. Trolox standard curve for (a) DPPH assay (b) ABTS assay

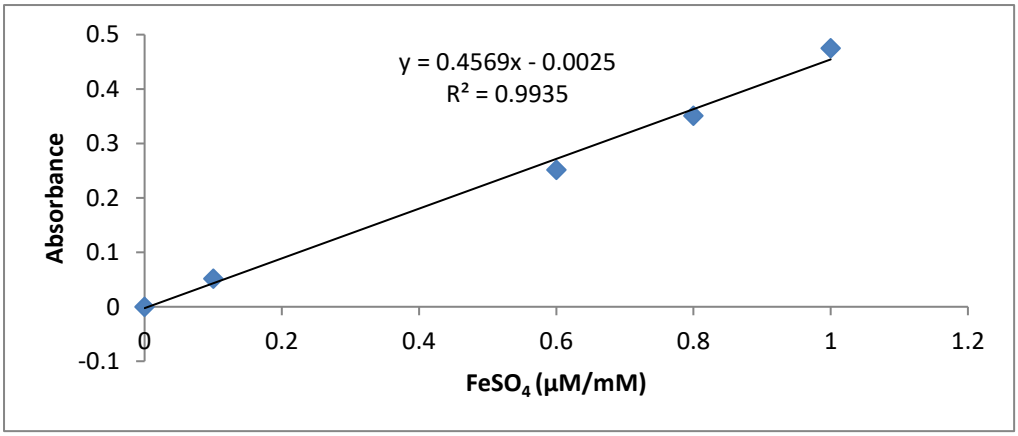

Figure 40. Ferro sulphate standard curve for FRAP assay

Appendix 11

Antioxidant Assay (cont.)

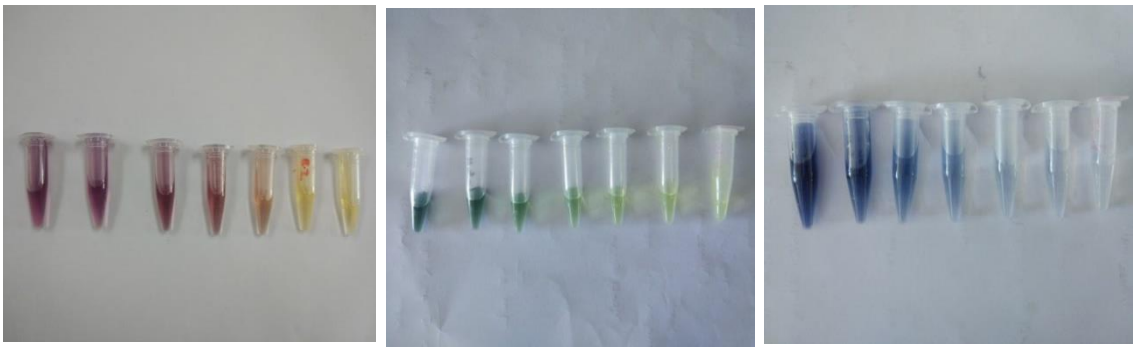

Figure 41. Antioxidant assay (a) DPPH assay with trolox standard (7.8125-500 mg/L)
(b) ABTS assay wit trolox standard (7.8125-500 mg/L)
(c) FRAP assay with FeSO4 standard (0.1-1 mM)

Appendix 12

Cytotoxicity Assay

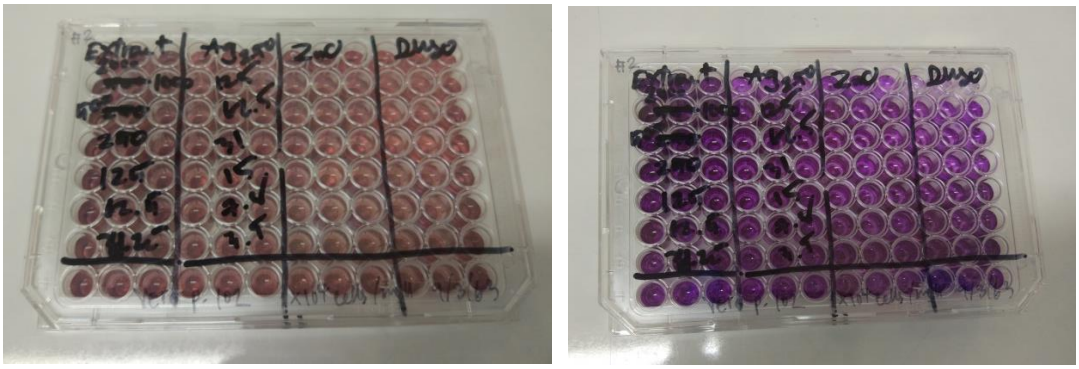

(a) (b)

Figure 42. MTT Assay for Vero cell (a) before treatment (b) after treatment

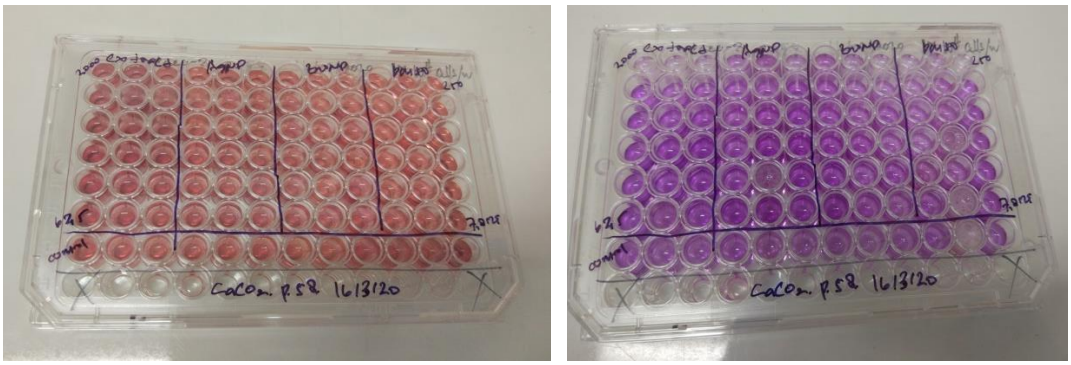

(a) (b)

Figure 43. MTT Assay for Caco-2 cell (a) before treatment (b) after treatment

VITAE

Name **Ms. Selly Arvinda Rakhman**

Student ID **6120320302**

Education Attainment

Degree	Name of Institution	Year of Graduation
B.Sc. (Chemistry)	Gadjah Mada University	2016

Scholarship Awards during Enrollment

1. Thailand's Education Hub for Southern Region of ASEAN Countries (TEH-AC) Scholarship Awards for Master's studies (2017) from Graduate School, Prince of Songkla University, Thailand.
2. Research Grant Scholarship from Graduate School, Prince of Songkla University, Thailand.

List of Publications and Conferences

Green Synthesis of Silver Nanoparticles (AgNP) using *Mimusops elengi* L. *Leaf* Extract and Its Antioxidant Activity, Oral Presentation, The 30th National Conference of Thaksin University in 2020 and the 1st National Conference of the Faculty of Humanities and Social Sciences, 30th May 2020.